

**DEVELOPMENT OF SUPPORTED METAL
CATALYST USING WASTE RESOURCES:
APPLICATION TO SYNTHESIS OF GLYCERYL
ESTERS**

THESIS

Submitted by

BIPIN KUMAR

[Exam. Roll No. M4CHE1608]
[Class Roll No. 001410302013]
[Reg. No. 128887 of 2014-2015]

Under the Guidance of

Dr. Rajat Chakraborty

(Associate Professor)

*In fulfillment for the award of the degree
of*

MASTER OF CHEMICAL ENGINEERING

**DEPARTMENT OF CHEMICAL ENGINEERING
JADAVPUR UNIVERSITY
Jadavpur, Kolkata-700032**

MAY 2016

Declaration of originality and compliance of academic ethics

I hereby declare that this thesis contains literature survey and original research work by the undersigned candidate, as part of his “*Master of Chemical Engineering*” studies.

All information in this document have been obtained and presented in accordance with academic rules and ethical conduct. I also declare that, as required by these rules and conduct, I have fully cited and referenced all material and results that are not original to this work.

Name: Bipin Kumar

Examination Roll Number: M4CHE1608

Thesis Title:

Development of supported metal catalyst using waste resources: Application to synthesis of glyceryl esters.

Signature:

Date:

MAY 2016

CERTIFICATION

This is to certify that Mr. Bipin Kumar, final year Master of Chemical Engineering (M.E) examination student of Department of Chemical Engineering, Jadavpur University (Exam Roll: M4CHE1608; Regd. No.:128887 of 2014-2015), has completed the Project work titled “Development of supported metal catalyst using waste resources: Application to synthesis of glyceryl esters” under the guidance of Dr. Rajat Chakraborty during his Masters Curriculum. This work has not been reported earlier anywhere and can be approved for submission in partial fulfillment of the course work.

Prof. (Dr.) Chandan Guha
*Head of Department and Professor,
Chemical Engineering Department
Jadavpur University.*

Dr. Rajat Chakraborty
*Project Supervisor,
Associate Professor,
Chemical Engineering Department
Jadavpur University.*

Prof. Sivaji Bandyopadhyay
*Dean of Faculty and Engineering
Technology
Jadavpur University.*

DEDICATION

*Special Dedication to my parents, friends and my
Respected project supervisor.*

For all your care, support and believe in me.

ACKNOWLEDGEMENT

First of all I thank almighty GOD for all His blessing.

In preparing this thesis, I have worked with a great number of people whose contribution in assorted ways to the research and the making of the thesis deserved special mention. It is a pleasure to convey my gratitude to all of them in my humble acknowledgment

I would like to express my profound gratitude to Dr. Rajat Chakraborty for his supervision, advice, and guidance from the very early stage of this research as well as giving me extraordinary experiences throughout the work. Above all and the most needed, he provided me unflinching encouragement and support in various ways.

I am very grateful to Prof. (Dr.) Chandan Guha, Head of the Department, Chemical Engineering Department and all other faculty members for their help and cooperation. I would also like to offer my acknowledgements to staff members of my department. I am also indebted to Jadavpur University, Dept. of Chemical Engineering for support and giving me the opportunity to use the equipments to do my research.

I am very much thankful to my PhD senior Ms. Punam Mukhopadhyay for her continuous support, valuable guidance and encouragement at various stages of the project period.

My fellow friends should also be recognized for their support. My sincere appreciation also extends to all my colleagues and others who have provided assistance at various occasions. Their views and tips are useful indeed. Unfortunately, it is not possible to list all of them in this limited space.

Finally I would like to thank to my family for their excellent support and try to keep me high spirited throughout the master degree programme.

TABLES OF CONTENTS

Chapter Title	Page No.
1. PREFACE	1-2
2. INTRODUCTION	3-15
2.1 Catalyst Development from Waste Resources	4-15
2.1.1 Energy scenario: Fossil fuel	5-6
2.1.1.1 Harmful Exhaust Emission of Diesel Fuel	5-6
2.1.2 Renewable Fuel: Biodiesel	7-8
2.1.2.1 Physical Properties of Biodiesel	7-8
2.1.2.2 Disadvantage Related to Biodiesel	8
2.1.3 Different Fuel Additive	9-15
2.1.3.1 Glycerol: Its history & application	10-12
2.1.3.2 Glycerol Transformation into Fuel Additive	13-15
3. LITERATURE REVIEW	16-33
3.1 Synthesis of Glycerol Based Fuel Additives Using Solid Acid Catalysts	17-32
3.1.1 Synthesis of Valuable Esters Using Homogeneous Catalyst	17-21
3.1.1.1 Different Glycerol Based Fuel Additive Esters Using Heterogeneous Catalyst	18-21
3.1.2 Different intensification methods	21-23
3.1.2.1 Microwave Activation	21-22
3.1.2.2 Ultrasonic Activation	22

3.1.2.3 Infrared Activation	23	
3.1.3 Waste Management and its utilization	23-24	
3.1.4 Cost Effective Catalyst Using Waste Resources	24-29	
3.1.4.1 Chemical Preparation of HAp & its Applications	24-26	
3.1.4.2 Preparation of HAp from Natural Resources	26-27	
3.1.4.3 Application of Hydroxylapatite (HAp) as a Catalyst & Catalyst Support	27-29	
3.1.5 Present Work: Literature Review	29-32	
3.1.5.1 Diacetin and Triacetin Synthesis	29	
3.1.5.2 Antimony as Catalyst	30-32	
3.1.5.4 Optimization Study using Taguchi Design	32	
3.2 Ethyl Hexyl Acetate as Fuel Additive	32-33	
4. AIMS AND OBJECTIVES	34-35	
5. MATERIALS AND METHODS	36-40	
5.1 Reagents and Materials	37	
5.2 Pork bone Processing	37	
5.3 Experimental Design	37-38	
5.4 Catalyst Characterization	39	
5.5 AA-G esterification using Sb_PHAp catalyst	39-40	
5.6 Reusability protocols for catalyst	40	
5.7 Engine Performance Test	40	

6. RESULT AND DISCUSSIONS	41-73	
6.1 Glycerol acetic acid esterification with pork bone supported antimony HAp catalyst	42-64	
6.1.1 ANOVA Study and Optimal Condition Evaluation	42-43	
6.1.2 Contour plot	44	
6.1.3 Effect of Process Parameters on DT Yield	45-48	
6.1.3.1 Effect of AA:G Mole Ratio	45	
6.1.3.2 Effect of Temperature	45-46	
6.1.3.3 Effect of Catalyst Concentration	46	
6.1.3.4 Effect of Sb precursor loading	46-47	
6.1.3.5 Effects of Reaction Time	47-48	
6.1.3.6 Effects of IR Activation at optimal condition	48	
6.1.4 Catalyst Characterization	49-55	
6.1.4.1 TGA Analysis	49	
6.1.4.2 FTIR Analysis	50	
6.1.4.3 XRD Analysis	51-52	
6.1.4.4 BET Analysis	53	
6.1.4.5 SEM Analysis	53-54	
6.1.4.6 Catalyst Recycling	54-55	
6.1.5 Probable Reaction Mechanism	55-56	
6.1.6 Fuel Property Evaluation	56-57	
6.1.7 Engine Characteristics	57-61	

6.1.7.1 Engine Emission	57-58	
6.1.7.2 Variation of engine emission with engine speed	58-60	
6.1.7.2.1 Carbon monoxide (CO) emission	58	
6.1.7.2.2 Carbon dioxide (CO ₂) emission	59	
6.1.7.2.3 Hydrocarbon (HC) Emission	59-60	
6.1.7.2.4 Nitrogen oxide (NO _x) Emission	60	
6.1.7.3 Engine Performance Analysis	61	
6.1.8 Variation of Engine Performance with engine Speed	62-64	
6.1.8.1 Brake specific fuel consumption (BSFC)	62	
6.1.8.2 Brake Thermal Efficiency (BTE)	62-63	
6.1.8.3 Heat Input (HI)	63	
6.1.8.4 Exhaust Gas Temperature (EGT)	63-64	
6.2 Performance and emission analysis of diesel engine fuelled with biodiesel & biodiesel-additive blends (2-Ethyl hexyl acetate and Triacetin)	65-73	
6.2.1 Comparative study on fuel properties of biodiesel and blended biodiesel	65-68	
6.2.1.1 Effect on Flash point	65	
6.2.1.2 Effect on Pour point	65-66	
6.2.1.3 Effect on Cetane number	66	
6.2.1.4 Effect on Density	66-67	
6.2.1.5 Effect on Viscosity	67-68	
6.2.1.6 Effect on Acid value	68-73	

6.2.2 Comparative study on diesel engine emission fuelled with biodiesel and blended biodiesel	68-71	
6.2.2.1 Carbon monoxide (CO) emission	69	
6.2.2.2 Carbon dioxide (CO ₂) emission	69-70	
6.2.2.3 Nitrogen oxide (NO _x) emission	70	
6.2.2.4 Hydrocarbon (HC) emission	70-71	
6.2.3 Comparative study on engine performance fuelled with biodiesel and blended biodiesel	71-73	
6.2.3.1 Exhaust Gas Temperature (EGT)	71-72	
6.2.3.2 Brake Thermal Efficiency (BTE)	72	
6.2.3.3 Brake Specific Fuel Consumption (BSFC)	72-73	
7. CONCLUSION	74-75	
7.1 Glycerol acetic acid esterification with pork bone supported antimony HAp catalyst	75	
7.2 Emission and performance study of diesel engine fuelled with TA-EHA-Biodiesel blend	75	
8. FUTURE SCOPE OF WORK	76-77	
9. REFERENCES	78-95	
Appendix I Abbreviations	96	
Appendix II List of figures	97-98	
Appendix III List of tables	99	
10. RESEARCH ACTIVITY	100	

CHAPTER-1

PREFACE

1. PREFACE

1.1 In this present study (first work) glycerol with acetic acid esterification has been conducted in an infrared irradiation aided batch reactor for maximization of combined selectivity of diacetin and triacetin using cost effective pork bone derived hydroxyapatite supported antimony (Sb) oxide catalyst (Sb-HAp). Under derived optimal condition of 40% Sb precursor loading at 100°C reaction temperature and 6:1 AA:G mole ratio resulted in maximum diacetin and triacetin yield. XRD, FTIR, SEM, BET-BJH and TGA analyses were performed to characterize the developed catalyst. The catalyst showed appreciable specific surface area: 40 m²/g; pore volume: 0.0485 cc/g and mesoporosity of 78% along with prominent crystalline phase of Sb₂O₅. Furthermore, diacetin & triacetin yield in conventional heating system (DT yield: 24%) indicated remarkable superiority of infrared irradiation (DT yield: 60%) on product specificity within 1h of reaction time. Additionally, the application of synthesized product as additive to palm biodiesel evinced 50% CO emission and 20% HC emission reduction coupled with 2 degrees depreciation in pour point. .

1.2 In the present work (second work) diesel engine emission and its performance has been tested using three different blends of triacetin and 2-ethyl hexyl acetate with palm biodiesel and their effect on biodiesel property has been studied by performing these tests viz. flash point, pour point, cetane number, density, viscosity and acid values. These additives have shown remarkable effect on pour point and NO_x emission resulting in a reduction of 4°C and 74% respectively. However very little improvement has been observed in terms of emissions and other engine performance parameters (brake specific fuel consumption and brake thermal efficiency. Thus this can be attributed to the fact that a single additive cannot improve all the fuel properties therefore, a blend of additives can be used to amplify the fuel performance.

CHAPTER-2

INTRODUCTION

2. INTRODUCTION

A catalyst is defined as a substance which increases or decreases the rate of reaction without getting consumed in the process. In recent years, the field of catalyst has seen a surge for development of cost effective catalyst derived from low cost materials mainly waste materials. Using waste material to develop the catalyst as well as the target product makes the overall process more cost effective and environmentally friendly. Below we have discussed about utilization of various waste and their transformation into cost effective valuable product.

2.1 Catalyst Development from Waste Resources

Various reports show that increasing number of researches are being done to prepare heterogeneous catalysts from waste materials. In recent time heterogeneous catalyst are being derived from various waste resources viz. fly ash, egg shells, fish scales, oyster shell, mollusk shell, shrimp shell, mud crab shell, turtle shell, clay which make the overall catalyst production cost effective. In addition to cost effectiveness utilization of these waste are proving an opportunity for better waste management. As each year millions of tones of solid waste are generated so catalyst development from these wastes can provide a better solution in order to mitigate environmental pollution and high cost of catalyst production. Fly ash is a waste material produced from coal based power plants, brick kilns and coal industry. Reports show that it has got wide field of application ranging from brick industry, cement industry, tiles industry and in road construction. In recent year municipal waste specifically slaughter house waste has gained significant attention of researchers. A slaughter house waste consists of 10-15% bone which is a source of natural hydroxylapatite. Primarily hydroxylapatite is synthesized chemically but it is not cost effective. Thus synthesis of natural hydroxylapatite has opened a new avenue. But compared to chemically synthesized HAp very scanty works have been reported using naturally synthesized HAp. Report says that naturally synthesized hydroxylapatite can be used as a cost effective

catalyst as well as catalyst support for various chemical process. Thus in the present work an attempt has been made to develop cost effective catalyst using natural HAp derived from pork bone to valorize glycerol to produce valuable ester preferentially fuel additives. In the subsequent section we will also discuss about disadvantages of fossil fuel primarily diesel, biodiesel as a potential renewable energy source, its inferior quality and combating them using suitable fuel additives.

2.1.1 Energy scenario: Fossil fuel

In this modern age fossil fuel being considered as the primary source of energy for almost all form of work ranging from transportation sector, agricultural field to industrial sector and also full filling various human needs. This fossil fuel being non renewable in nature, its reserved is limited and depleting day by day. Hence the focus of researchers and scientists across the globe is shifting towards more promising alternative fuel. Researchers from every corner of the world are over stretching themselves to find an alternative fuel that could completely replace fossil fuel which is nonrenewable and releases harmful emission .Due to the limited reserve of fossil fuel, renewable fuels are gaining momentum and becoming more attractive. Thus, in this section we have made an effort to identify inferior emission quality and their harmful effect on environment and human life.

2.1.1.1 Harmful Exhaust Emission of Diesel Fuel

Being the back bone of modern age, machinery to automation to agriculture, diesel is the primary energy source. Diesel is a mixture of hydrocarbons and it is produced from the distillation of crude. Diesel emanates harmful emissions viz., carbon monoxide (CO), hydrocarbon (HC), nitrogen oxide (NO_x), sulphur dioxide (SO₂) and smoke etc (*Votsmeier et al., 2005*). A detailed description of different physical properties of diesel has been given in [Table 2.1](#) (*Fernando et al., 2006*).

Table 2.1: Physical properties of diesel

Diesel Parameters	Units	Parameter Values
Density	Kg/m ³	845
Pour Point	°C	-10
Flash Point	°C	61
Cloud Point	°C	-15 to 5
Cetane Index	-	46
Cetane Number	-	51
Kinematic Viscosity	mm ² /s	1.9-4.1

Furthermore, the smoke basically contain two parts: solid particulate matter and organic component. These organic compounds present in the smoke of diesel emission are minor in quantity. These components are heavy organic compounds in nature and they posses serious threats to human health viz. PAH, aldehydes etc. A detailed description has been elaborated in [Table 2.2](#) encountering different harmful components of diesel emission that may endanger human health and our environment (*Nauss et al., 1995*). Apart from carbon dioxide (CO₂) which is a major contributor of global warming, all other components are immensely harmful to human health.

Table 2.2: Diesel Emission Constituents and their impact

Emission Constituent	EN Standard(g/kWh)	Impact
Formaldehydes	-	Carcinogenic in nature
Hydrocarbons (HC)	0.55	Causes respiratory irritation, carcinogenic in nature
Sulpher dioxide(SO ₂)	-	Causes respiratory irritation, causes acid rain
Nitrogen oxides(NO _x)	3.5	Causes respiratory irritation, causes acid rain
Carbon dioxide(CO ₂)	-	Causes global warming
Carbon monoxide(CO)	4.0	Poisonous to human, it blocks oxygen supply to body

2.1.2 Renewable Fuel: Biodiesel

Renewable energy sources are the next best alternative to fossil fuel and at the same time these renewable energy sources possess almost no threat to environment unlike fossil fuel. One of the appealing and attractive renewable fuel sources is biodiesel. Biodiesel is fundamentally the mono alkyl esters of vegetable oil or animal fats (*Sharma et al., 2014*). Transesterification of vegetable oil or animal fat with an alcohol produces methyl ester which is known as biodiesel along with glycerol as a by-product. The major advantage of biodiesel over diesel is its environmental friendly nature, its emission is on lower side than diesel. Additionally, particulate matter emission from biodiesel is much lesser than conventional diesel, also carbon related emission viz. carbon monoxide (CO), hydrocarbon (HC), carbon dioxide and other greenhouse gases from biodiesel combustion are quite less in comparison with diesel. Therefore, biodiesel can be considered as nontoxic and biodegradable coupled with its superior emission characteristics. In addition to this, biodiesel can be blended with diesel in any proportion and it can be used in most of the existing diesel engine without any upgradation. However biodiesel also acquires certain pitfalls which have been covered under the subsequent section.

2.1.2.1 Physical Properties of Biodiesel

Biodiesel possesses higher viscosity, molecular mass, pour point and density than its contemporary diesel fuel (*Hoekman et al., 2012; Silitonga et al., 2013; Ashraful et al., 2014*). Having higher viscosity and molecular mass, these result in unfavorable conditions during engine operations viz. poor volatility, carbon deposition inside injector, poor atomization and finally rendering incomplete combustion of biodiesel (*Bagboy et al., 1987*). A detailed description of different physical properties of biodiesel has been tabulated in [Table 2.3](#) (*Vedaraman et al., 2011; Mofisur et al., 2012; Fattah et al., 2014*) to understand its limitations.

Table 2.3: Physical Properties of biodiesel

Biodiesel Properties	Units	Values	Standard Methods
Density	kg/m ³	880	ASTM D 4052
Pour Point	°C	13-16	ASTM D 97
Flash Point	°C	160	ASTM D 92
Cloud Point	°C	14-17	ASTM D 2500
Calorific Value	mj/kg	38.69	ASTM D 240
Cetane Number	-	50-52	ASTM D613
Viscosity at 40°C	mm/s ²	3.94	ASTM D 445
Oxidation Stability	-	7.2	ASTM E 2412

2.1.2.2 Disadvantage Related to Biodiesel

From [Table 2.3](#), it is quite evident that some of its properties may cause difficulties in using biodiesel as an effective fuel in cold climate. Indistinctly, in cold climate, due to higher pour point of biodiesel than conventional diesel fuel it may clog the engine filters resulting engine shut down. To address this issue, winterization technique has been employed which has been expected to improve biodiesel cold property. Furthermore, due to poor oxidation stability, shelf life of biodiesel is shorter than diesel, also nitrogen oxide emission from biodiesel (particularly from palm biodiesel) combustion is quite high than diesel. Therefore, for last few years, to promote biodiesel production in need for greener fuel researchers are focusing on the development of suitable fuel additive that not only counteracts the limitation of biodiesel but could also enhance its fuel property thus, making biodiesel competent with diesel. This can be well achieved via using surplus glycerol from biodiesel industry to generate an effective fuel additive.

2.1.3 Different Fuel Additive

Fuel additives are the chemical substances which are used to improve or enhance the certain properties of a fuel. According to their use fuel additives could be mixed with gasoline/petrol (*Wang et al.,2004*), diesel, biodiesel (*Ribeiro et al.,2007*) and aviation fuel in a proportion of less than 1%. Fuel additive is a chemical substance that helps in achieving better engine performance by keeping engine and its parts clean and prevents incomplete combustion which leads to better and improved engine efficiency, less emission of green house gases and harmful particulate matter as well as fuel additive also protects engine parts from corrosion which results in better engine life (*Chevron 2009*). Addition of fuel additive and alcohol to diesel significantly reduce the particulate emissions (*Rakopoulos et al.,2008*) whereas fuel additive addition to marine diesel fuel results in significant reduction in carbon dioxide (CO₂), nitrogen oxide (NO_x) and particulate emission, and improves concentration of oxygen and excess air quantity (*Lin et al.,2006*). For better jet engine performance fuel additive is mixed in 1-70% concentration, it minimizes the depositions in jet engine and enhances the thermal stability (*Forester et al., 2003*). The use of fuel additives and its wide field of application have been summarized below.

- ❖ Improves cold flow property of biodiesel.
- ❖ To meet fuel specification it is mixed with diesel/gasoline.
- ❖ Protects pipe lines, fuel tanks, engines from corrosion.
- ❖ Increases shelf life of fuel and fuel could be stored for a longer time.
- ❖ Reduces pumping cost in fuel pipe lines.
- ❖ Reduces emission and enhances engine performance by keeping engine clean.

Depending upon application fuel additives can be classified as follows. Cold flow improver namely ethanol, polymethyl acrylate (PMA), which enhances the cold weather operability of biodiesel, whereas oxygenated additive helps in better combustion and produces minimal pollutants. Antioxidant additive prevents gum formation in biodiesel by stopping polymeric chain reaction and improves stability in storage. Few antioxidants are as follows: pyrogallol (PL), propyl-gallate (PG), hydroxyanisole (BHA) (*Sohober et al., 2004; Karavalakis et al., 2011; Joshi et al., 2013*). Lubricity improver 1,2-ethanediol, 1,3-propanediol and 1,2,3-propanetriol helps in improving service life of engine and its parts by minimizing friction (*Batt et al., 1996*). Metal based additive such as NiO, MnO₂ or MgO improves engine performance and reduces exhaust emission (*Joshi et al., 2007*). Cetane number improver reduces ignition delay, diesel consumption, exhaust emission and enhances engine performance these include mainly 2-ethylhexyl nitrate, cyclohexyl nitrate and 2-methoxyethyl ether (*Ullman et al., 1994; Lu et al., 2005*).

2.1.3.1 Glycerol: Its history & application

The history of glycerol takes us back to around 2800 BC, when it was produced from the saponification of fats (*Christoph et al., 2006; Pagliaro et al., 2007*). The word glycerol is derived from the word “glycos” a Greek word means “sweet”. Sometimes it is also called as sugar alcohol. Till 20th century glycerol was produced as a byproduct of soap industry. There are various ways to produce glycerol either by synthetic route or as a by-product of biodiesel production. Glycerol is produced as a waste product or as a by-product in biodiesel industry, which is basically 10 wt% of total bio-diesel produced (*Malero et al., 2012*). In Europe since 2000 there is a jump of 28% in biodiesel production and it has reached 5 million metric tons (MTm) of biodiesel production in 2006 (*Malero et al., 2008*) whereas in US, from their existing biodiesel production capacity of approximately 300 million gallons per year (gpy) they want to reach 600 million gpy in next few years (*Bowman et al., 2006*). To meet the Kyoto

protocol Canada aimed to produce 500 million litres/year of biodiesel by the year 2010 (*Smith et al., 2009*) whereas Malaysia is targeting to reach a biodiesel production 500,000 tone per year (tpy). The international biodiesel production trend shows that now countries are focusing more towards greener and cleaner fuel and this leads to an increased production of biodiesel and as a result a huge amount of surplus glycerol is also produced as a by-product. This surplus glycerol is of 80-88% purity (*Pramanik et al., 2005*). The current market is unable to absorb this surplus glycerol and in addition to this crude glycerol needs to be purified for industrial grade of 98% (*Kenkal et al., 2008*). A report by Tyson (2003) indicated that due to this surplus glycerol production cost production of biodiesel could also be dropped from US\$ 0.63 per liter to US\$ 0.38 per liter (*Paliagro et al., 2008*). Below given Fig. 2.1 (*Yazdani et al., 2007*) shows how over the years surplus glycerol is produced from biodiesel industry and it leads to the gradual fall in glycerol price. This condition would give rise in a situation where glycerol will not be profitable for biorefiners and it will be considered as a waste (*Kolmetz et al.,2005*) and it will also create storage and disposal problem in environment (*De-silva et al.,2009*).

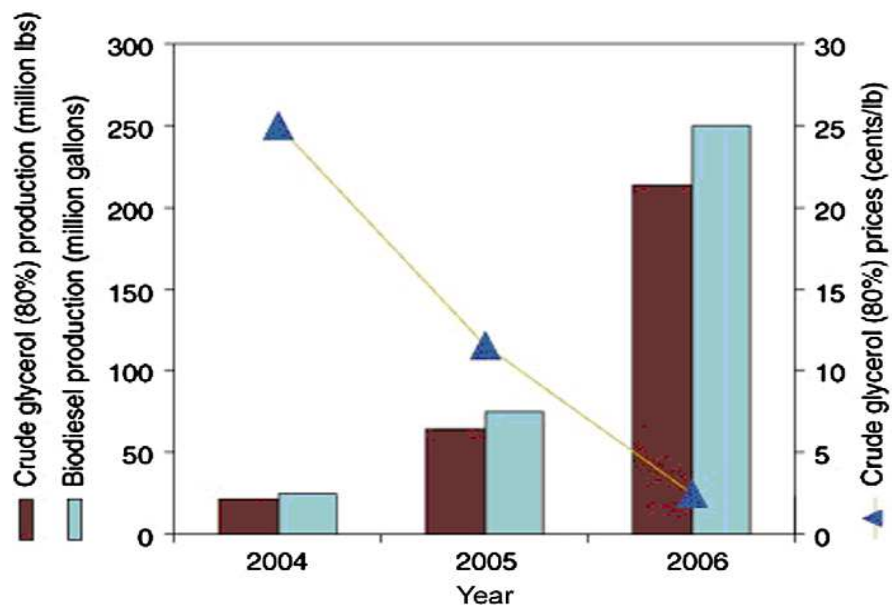


Fig. 2.1: Increasing production of biodiesel and crude glycerol lead to plummeting glycerol price

Glycerol being colorless, transparent, odorless, non toxic, and sweet in nature, it has got wide range of application in different field of life viz. in food & beverage industry, in beauty cosmetic products, in pharmaceutical industry, in chemical industry, in tobacco and resin industry etc. The existing market of glycerol and its consumption pattern is represented below in Fig. 2.2 (Paglirao et al., 2007).

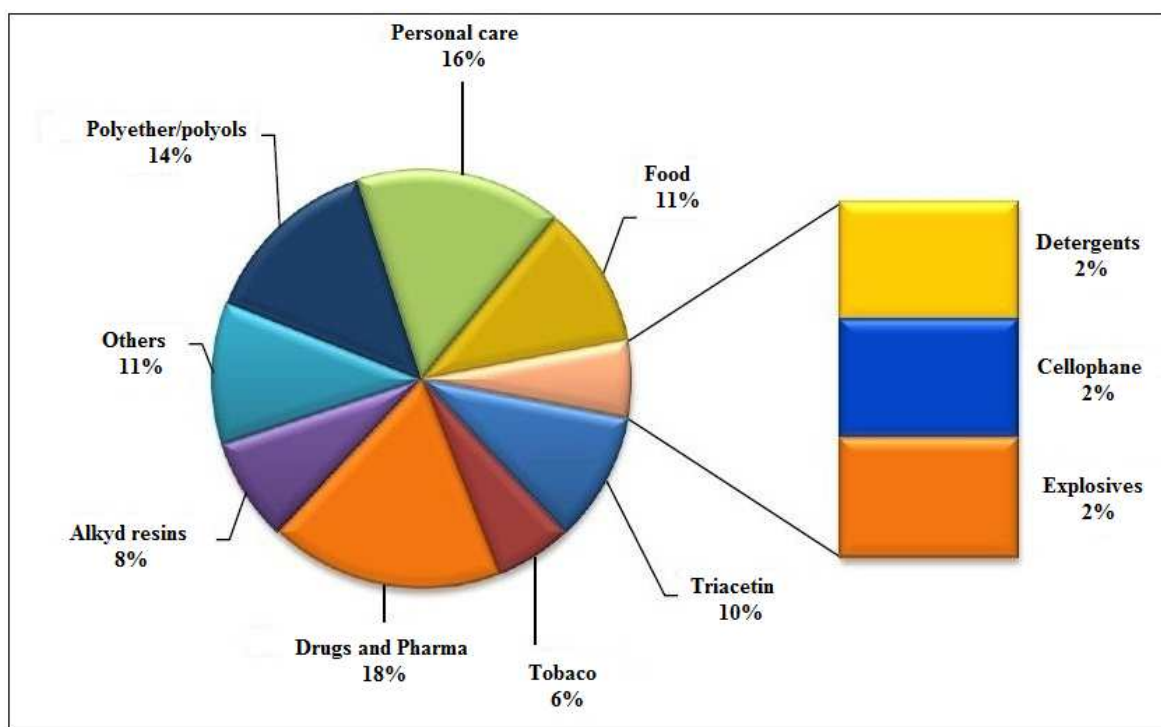


Fig. 2.2: Industry wise application of glycerol

The pie chart clearly shows that majority of the glycerol is consumed by pharmaceutical industry, food & beverage industry, and beauty care industry as 18%, 11% and 16% respectively. Some other industry viz. tobacco, detergent, explosive etc also consume a little amount of glycerol. But analyzing the market trend of glycerol consumption it can be well said that existing market is immature to consume the surplus glycerol coming out from fast growing biodiesel industry. To valorize this excess glycerol various researches have been carried out in order to transform the low value glycerol by different

strategies and approaches. Thus, the present researchers are concentrating on transformation of glycerol into fuel additives that could be used in fuel industry.

2.1.3.2 Glycerol Transformation into Fuel Additive

In present years, glycerol has gained immense attention for fuel additive synthesis. Conversion of glycerol to valuable fuel additives is achieved through various chemical routes viz. esterification, acetylation or etherification and many others which have not been covered in the present thesis. The reason behind its conversion is that, it cannot be directly added to fuel because of its polymerizing and degrading nature. Thus, this could result in consequential engine problems at high temperatures. Hence glycerol is being transformed into effective fuel additive that will not only enhance fuel property but can also control exhaust emissions from diesel and biodiesel. A property comparison (*Clnakci et al., 2003*) has been summarized in [Table 2.4](#) to understand the applicability of diesel and biodiesel in CI engine.

Table 2.4: Fuel property comparison between diesel and biodiesel

Fuel Property	Diesel (ASTM D975)	Biodiesel (D6751)
C/H ratio	6.82	6.53
Sulfur (wt. %)	0.041	0.0 to 0.005
Oxygen (wt. %)	0	11
Carbon (wt. %)	87	77
Hydrogen (wt. %)	13	12

The comparative study of properties between diesel and biodiesel shows that biodiesel has higher oxygen (O₂) contents and lower carbon (C) value and it leads to better combustion in an engine and

lower exhaust emission except nitrogen oxide (NO_x) emission which is on the higher side. However, this issue could be well addressed by using proper fuel additive. Below some of the glycerol derived fuel additives are given in [Table 2.5](#).

Table 2.5: Glycerol based additives

Glycerol based additive	Application	Reference
Polyglycerol	Improves lubricity in chocolates	Clacens et al.,2002
Glycerol Diacetate	Improves cold flow property & viscosity of biodiesel	Melero et al.,2007 Goncalves et al.,2008
Glycerol Triacetate	Use to improve antiknocking property of gasoline and improves viscosity of fuel	Luque et al.,2008 Ferreira et al.,2009
Glycerol Acetal	Imparts oxidative stability to fuel	Garcia et al.,2008
Di-tert-Butyl glycerol ether & Tri-tert-butyl glycerol ether	Reduce viscosity, improve cold flow property, reduce particulate emission, green house gas emission and unregulated aldehyde in exhaust	Noureddini et al.,1998 Klepacova et al.,2007 Jamroz et al.,2007 Melero et al.,2008

Glycerol emerges as a significant worth chemical that can be converted into high value products. In the prospect of world wide energy scenario glycerol has great demand towards renewable sources, glycerol has proved to have tremendous potential to be transformed, thus supersede conventional petroleum derived fuel additive. Many glycerol based esterification products such as diacetyl glycerol, triacetyl

glycerol, and glyceryl monooleate have been identified as potentially valuable additives for diesel, gasoline, biodiesel and blend biodiesel-diesel. Thus, the present researchers are concentrating on transformation of glycerol into fuel additives that could be used in fuel industry. Accordingly, in our present work, emphasis had been given on the production of a valuable additive that will finally generate proficient fuel rendering higher fuel efficiency and better engine performance. The upcoming chapter will give us an overview of the production of such glycerol based fuel additives and their applications in diesel engine. The upcoming chapter will also encompass the preparation method of these valuable esters through catalytic route.

CHAPTER-3

LITERATURE REVIEW

3. LITERATURE REVIEW

3.1 Synthesis of Glycerol Based Fuel Additives Using Solid Acid Catalysts

A detailed review has been performed in the following section to understand the utility of glycerol for production of valuable fuel additives and its performance when blended with diesel or biodiesel. Furthermore, this literature review also encompasses different heterogeneous catalyst involved in fuel additive synthesis

3.1.1 Synthesis of Valuable Esters Using Homogeneous Catalyst

A catalyst which remains in a reaction system soluble with the reactants i.e. in a same phase with reactants is called homogeneous catalyst. Homogeneous catalysts are alternative to heterogeneous catalysts. Homogeneous catalysts are employed in various applications because of their unique selectivity and conversion towards targeted products. For the production of valuable esters homogeneous catalyst are also employed. Some of the valuable esters produced using homogeneous catalyst are glycerol ketals, glycerol acetates and branched alcohol-derived fatty esters. Glycerol ketal (solketal) is a synthesised product of glycerol and acetone and it is a well-known oxygenated fuel additive. To catalyze this reaction various Bronsted acid viz. phosphoric acid, sulfuric acid, hydrochloric acid or p-toluene sulfonic acid are used as a catalyst (*Girald et al., 2009*). Another important ester glycerol acetate which is extensively used as a fuel additive is synthesized from the esterification of glycerol and acetic acid. The reaction has been catalyzed by p-toluene sulfonic acid with good productivity of monoacetates, diacetates and triacetate as 40 wt.%, 27 wt.% and 33 wt.% respectively (*Girald et al., 2009*). Therefore, despite having a unique selectivity and conversion homogeneous catalysts are still losing shine in front of heterogeneous catalyst. This can be attributed to the fact that separation of homogeneous catalyst from final reaction mixture and its disposal incurs additional cost

and may result environmental problems. In subsequent sections we will be thus discussing about heterogeneous catalyst and their application in synthesis of valuable fuel additives from glycerol.

3.1.1.1 Different Glycerol Based Fuel Additive Esters Using Heterogeneous Catalyst

Glycerol being a byproduct from biodiesel industry is significantly gaining importance all over the globe because of its availability in abundance and its non toxic nature. Crude glycerol has low market value that's why various researches are going on to convert glycerol as a value added product. In the last few year various researches have been carried out and as a result some of the valuable products have been identified as potential fuel additive viz. glycerol ether, glycerol acetal and acetyl glycerol. Glycerol based fuel additives are best alternative to existing fuel additives viz. methyl-tert-butyl ether (MTBE) and ethyl tert-butyl ether (ETBE). MTBE & ETBE are made from petroleum feed stoke and various findings say that they cause health problems in human and animals and they are also known to pollute underground water and aquatic life. Therefore, to synthesize valuable fuel additives using glycerol various heterogeneous catalysts have been studied which has been tabulated in [Table 3.1](#) to identify the research gap in the present research articles.

Table 3.1: Glycerol based fuel additives

Name of Glycerol derived additive	Catalyst	Reaction conditions	Remarks	Uses	Reference
Diglyceride & Triglyceride of Acetic acid	Sulfonic acid-modified SBA-15	Temp. 125°C, Time 4hr,G:AA 1:9 Combined selectivity of 85%	Longer reaction time coupled with higher molar ratio	Improve viscosity & cold flow property	Melero JA et al.,2007

Name of Glycerol derived additive	Catalyst	Reaction conditions	Remarks	Uses	Reference
Diglyceride & Triglyceride of Acetic acid	K-10 montmorillonite	Temp. 300°C, Time 30min, Conversion 96%; Combined selectivity 98% [TAG 5%]	High activation temperature & low Triacetyl glycerol selectivity	Improve viscosity & cold flow property	Goncalves VLC et al., 2008
	PMo(Dodeca molybdophosphoric acid) encaged in USY Zeolite	Time 3hr; Cat loading 1.9wt%; Combined Selectivity 61% [TAG 2%]	Longer reaction time & very low Triacetyl glycerol selectivity		Ferriera et al., 2009
	AgPW(Silver exchanged phosphotungstic acid)	Temp. 120°C; Time 15min.; G:AA 1:10; Cat loading 1wt%; Conversion 96.8%; Combined Selectivity 51.1%	High conversion but at the expense of high molar ratio and expensive catalyst		Zhu et al., 2013
	TPA(12-tungstophosphoric acid) anchored to MCM-41	Temp. 100°C; Time 6hr; G:AA 1:6; Cat 0.15gm; Conversion 87%; Combined Selectivity 75% [TAG 15%]	High temperature & longer reaction time; low Triacetyl glycerol selectivity		Patel & Singh, 2014
Glycerol Monocaprin	Carboxylesterasa	Time 15hr; Temp. 50°C, Selectivity 80%	Longer Reaction Time	Fuel Lubricant	Park et al., 2010
Glycerol Palmitate	Candida Antarctica lipase B	Temp. 50°C; Time 24hr; Conversion 90%; Selectivity 53%	Longer Reaction Time	Cetane Improver	Kapoor & Gupta, 2012

Table 3.2: Glycerol based fuel additives (Continued)

Name of Glycerol derived additive	Catalyst	Reaction conditions	Remarks	Uses	Reference
Glyceryl Monooleate	Zinc Oxide (ZnO)	Temp. 150°C;G:OA 4:1;6hr;conversion 90%;selectivity 80%;cat loading .5wt%	High reaction time and temperature	Fuel Lubricant & pour point depressant	Singh et al.,2013
Glyceryl Monolaurate	Zeolite	Temp. 100°C;Time 24hr;Yield 20%;Selectivity of GML 65%	High reaction time and a low yield	Fuel Lubricant	Machadoa et al.,2000
	Aluminium & Zirconium acid catalyst	Temp. 150°C;Time 18hr;Pressure 10 Mpa;Conversion of Lauric Acid (LA) 93%	High reaction time and temperature		Sathivel et al.,2007
	SBA-15	Temp. 160°C,Time 7hr;Conversion 90-95%	High temperature & longer reaction time		Hermida et al.,2011
	Mg-Al-CO ₃	Temp. 180°C; Time 2hr;Conversion of LA 99%	High temperature		Hemerski et al.,2014
	SBA-15	Temp. 160°C; Time 6hr;Conversion of LA 70%;Yield of GML 50%	High temperature and longer reaction time		Hoo & Abdullah,2014

Thus, from the above literature reviews it can be concluded that synthesis of these valuable esterified products require higher reaction temperature or longer reaction time for desired conversion and selectivity. Whereas in some cases higher molar ratios have been reported for the desired conversion

coupled with the employment of expensive catalysts. So there is a need of intensive study to optimize the reaction system to minimize these system constraints and maximize desired yield and selectivity in an energy efficient pathway.

3.1.2 Different intensification methods

In recent years much focus and attention is being given to save energy worldwide and the field of chemical engineering is not an exception. Researchers are continuously focusing on new energy saving methods and environmental friendly technology to improve reaction system and it has attracted attention of researchers to find new avenues to improve chemical processes. Literature review shows in the last two decades some intensification methods have been used in chemical processes (esterification, transesterification and etherification has been covered in the present thesis) and these have drawn increasing interest among researchers. These methods are given below.

- ❖ Microwave activation
- ❖ Ultrasonic activation
- ❖ Infrared activation

3.1.2.1 Microwave Activation

Microwave activation has been in large practice to intensify a chemical reaction. Microwave irradiation lies in between infrared and radio wave in electromagnetic spectrum. Microwave activation is known to improve energy efficiency on ground of highly focused energy to reaction system thus resulting in increased rate of reaction, better energy management and increased yield. Literature review shows that microwave activation has been employed in various chemical systems viz. esterification, transesterification. *Kiss & Keglevich (2016)* have reported to intensify the esterification of cyclic

phosphinic acids in the presence of ionic liquids using microwave irradiation and it has resulted in enhanced efficiency. In another work *Buasri et al. (2015)* has reported that application of microwave irradiation in transesterification of *Jatropha Curcas* oil has resulted in high biodiesel production in shorter time. Microwave irradiation for biodiesel production has resulted in higher conversion in esterification of free fatty acids as reported by *Lieu et al. (2016)*. Hence it can be concluded that application of microwave irradiation in chemical process saves time, energy, increases yield and conversion.

3.1.2.2 Ultrasonic Activation

Ultrasonic activation has shown promising results in intensification of various chemical reactions. It is known to enhance mixing and temperature of reaction mixture simultaneously. The ultrasonic activation which utilizes ultrasound as a tool to propel or accelerate the chemical reaction has emerged as a promising field of research in the synthesis of various chemical driven products with improved conversion, better performance and shorter reaction time. Many research articles have been reported during the last few years on ultrasonic activation of chemical processes which shows increasing interest of researchers and scientific community towards ultrasonic activation. Ultrasonic irradiation has resulted in better esterification performance in terms of esterification efficiency and reaction time for *Jatropha* oil than mechanical stirring and hand shaking mixing as reported by *Andrade-Tacca et al. (2014)*. In another case ultrasonic activation has resulted in increased rate of biodiesel production with shorter reaction time and lower reaction temperature as reported by *Maneechakr et al. (2015)*. *Hajamini et al. (2016)* has successfully employed ultrasound radiation in esterification of waste fish oil and it has resulted in reduced reaction time, lower molar ratio of alcohol to oil and improved energy consumption. Hence it can be said that ultrasonic activation is an attractive technique to improve chemical process performance.

3.1.2.3 Infrared Activation

Infrared irradiation is invisible part of a electromagnetic spectrum. It is further divided into three sub part near infrared (0.76–1.5m), middle infrared (1.5–5.6m) and far infrared (5.6–1000 m). Infrared irradiation can be used to intensify chemical reactions by virtue of its heating capacity. One of the main advantages of using infrared heating is its uniform heating which results in improved efficiency of a chemical process. It is being used as a heating source in many industrial applications viz. in glass industry for annealing, in plastic industry and in print drying. But particularly in the field of chemical process intensification infrared irradiation has got few applications. Very scanty work has been reported on infrared activation of chemical processes viz. esterification, transesterification or biodiesel production. *Chakraborty & Sahu (2014)* have utilized infrared assisted heating for biodiesel production using waste goat tallow and as a result it has accelerated the conversion process in shorter time resulting in maximized biodiesel yield compare to conventional heating. Infrared irradiation has been used in esterification between glycerol and lauric acid and it has rendered in higher conversion in shorter time period thus making the system energy efficient than conventional conductive heating system as reported by *Chakraborty & Mandal (2015)*. In another work infrared assisted biodiesel production from waste mustard oil has shown fast production of biodiesel compare to conventional heating and made the process cost effective by saving time and energy as reported by *Pradhan et al. (2016)*. Thus from the above literature review it can be concluded that its ability of uniform heating makes it a better option and so its application holds a promising future for process intensification of esterification reaction.

3.1.3 Waste Management and its utilization

Development of catalyst from waste resource is highly advantageous as it will lower the overall cost of production and at the same time it will solve the disposal problem of waste materials in environment.

Non efficient or under utilization of animal waste which mainly consist of bones, scales or egg shells and various body parts of animal will create environmental pollution, health problem and as well as disposal problem. Considering India which is world's largest house of farm animal viz. buffalos, goat, sheep and poultry and growing at a rate of 6% per annually (*Jayathilakan et al.,2012*). It produces huge amount of animal waste every year. A pig carcasses, beef carcasses and lamb carcasses consist of 11%, 15% and 16% of bone respectively. These bones are promising source of catalyst as well as catalyst support that could be utilized in the development and production of natural hydroxylapatite. Thus utilization of animal bones could help in better solid waste management.

3.1.4 Cost Effective Catalyst Using Waste Resources

The field of catalysis is on revival. In last few year various research has been carried out for the development and design of new catalyst derived from natural waste or low cost material. To prepare a cost effective heterogeneous acid catalyst a promising catalyst support has been considered that is hydroxylapatite (HAp). These support posses a promising ion exchange capacity, high adsorption capacity, distinctive acid base property and non toxicity. These catalysts can be prepared either via chemical route or can be derived from animal bones, scales or egg shells. In next part we will be discussing about synthesis of hydroxylapatite from chemical route as well as from natural waste resources.

3.1.4.1 Chemical Preparation of HAp & its Applications

Hydroxylapatite (HAp) is a widely available naturally occurring mineral calcium phosphate. Usually it is denoted by $\text{Ca}_{10}(\text{PO}_4)_6(\text{OH})_2$. It is found from study that hydroxylapatite has striking similarity with human hard tissue found in the bone. In industrial practice hydroxylapatite is synthesized via several chemical routes. Some of the well known methods are as follow.

- ❖ Wet Chemical Precipitation
- ❖ Sol-gel technique
- ❖ Hydrothermal technique
- ❖ Biomimetic deposition
- ❖ Electrodeposition technique

Among these methods the most popular and widely followed technique for hydroxylapatite synthesis is wet chemical precipitation. Sometimes also called as precipitation technique. This method was invented by Yagai and Aoki as reported by *Bouyer et al. (2000)*. This method utilizes calcium hydroxide ($\text{Ca}(\text{OH})_2$) and phosphoric acid (H_3PO_4) as the primary reaction material and apart from hydroxylapatite as a primary product this reaction leaves water as a produced.

Hydroxylapatite (HAp) has got wide range of application. Owing to its great similarity with human bone tissue it is widely used in medical field. The major application of hydroxylapatite that includes is given below (*Kantharia et al.,2014*).

- ❖ Dental coating & surgery
- ❖ Bone tissue engineering
- ❖ Toothpaste component
- ❖ Drug and gene delivery
- ❖ Packing material in column

Apart from these traditional applications new researches have opened various new fields where HAp is being considered as a potential game changer viz. to reduce exhaust emission hydroxylapatite is used in air filters and it is found to be very effective in absorbing and decomposing carbon monoxide (CO) (*Nasr-Esfahani et al.,2012*). In another new application hydroxylapatite-alginate complex were employed as an adsorbent to remove fluorides using ion exchange mechanism and added advantage with this composite material is its biodegradable nature and biocompatibility (*Pandi et al., 2014*). Some new researches have also showed its promising and potential use in the field of protein separation (*Potty & Xenopolous ,2011*). One major application which has emerged in recent time is in the field of catalysis. Many report suggest that hydroxylapatite (HAp) is being used as a catalyst and catalyst support successfully (*Okumara et al., 2013*). In subsequent section we will be discussing about preparation of hydroxylapatite from natural resources.

3.1.4.2 Preparation of HAp from Natural Resources

Although chemically synthesized hydroxypapatite (HAp) is widely used, in recent time naturally derived hydroxypapatite has drawn the attention of various researchers across the globe. Natural hydroxylapatite (NHAp) can also be prepared or derived from natural resources viz. fish scale, animal bone, bird bone and egg shell. *Chakraborty et al. (2014)* has successfully derived natural hydroxypapatite (NHAp) using turkey bone and employed it as a catalyst after calcination. This catalyst was further successfully employed to optimize the production of biodiesel from Indian mustard oil as reported by Chakraborty et al. Initially turkey bone was boiled in deionized water in order to remove flashy part and make it deproteinized. Then turkey bone was converted to finely powdered material in a ball mill using wet grinding technique to obtain natural hydroxylapatite and finally it is subjected to calcination to convert it to catalyst. Thus it can be concluded that naturally derived hydroxylapatite has exhibited very proficient

performance as a support and catalyst. In next section we will discuss about application of HAp as a catalyst and catalyst support in detail.

3.1.4.3 Application of Hydroxylapatite (HAp) as a Catalyst & Catalyst Support

Application of hydroxylapatite in the field of catalysis is a new avenue. The potential use of hydroxylapatite as a catalyst and catalyst support has drawn significant attention of researchers in recent time. A detailed literature review shows that various works have been reported using hydroxylapatite. [Table 3.3](#) has been provided to understand the application of (HAp) as an effective catalyst as well as promising cat support.

Table 3.3: Application of Hydroxylapatite (HAp) as a Catalyst & Catalyst Support

SL. No.	Year	Author's Name	Application	Catalyst Properties	
				BET Surface area (m ² /g)	Acidity/Basicity
1	2001	Sebti et al.	ZnCl ₂ /HAp lewis acid-catalyst for Friedel-Crafts Alkylation Reaction.	38.26 m ² /g	-
2	2002	Sebti et al.	HAp as a support in Knoevenagel Reaction.	38.26 m ² /g	-
3	2003	Zahouily et al.	HAp as an efficient catalyst in Michael's Addition Reaction.	38.0 m ² /g	-
4	2003	Venugopal & Scurrrell	Au-HAp catalyst in the water gas shift reaction.	54.0 m ² /g	-
5	2004	Mori et al.	Pd-HAp catalyst for oxidation of alcohols.	48.8 m ² /g	-

Table 3.4: Application of Hydroxylapatite (HAp) as a Catalyst & Catalyst Support (Continued)

SL. No.	Year	Author's Name	Application	Catalyst Properties	
				BET Surface area (m ² /g)	Acidity/Basicity
6	2010	Chakraborty et al.	Transesterification of soybean oil catalyzed by fly ash-HAp catalyst	0.701m ² /g	1.6 mmol HCl/g
7	2011	Chakraborty et al.	Biodiesel synthesis using low cost fish scale derived HAp catalyst	39 m ² /g	-
8	2011	Huang et al.	Au-HAp catalyst for low temperature CO oxidation	84 m ² /g	0.70 mmol CO ₂ /g
9	2012	Chakraborty & Das	Ni-HAp catalyst for esterification of free fatty acid	90 m ² /g	7.52 mmol NaOH/g
10	2013	Chakraborty & RoyChowdhury	Esterification of oleic acid using Cu-HAp	16.78 m ² /g	11.22 mmol KOH/g
11	2014	Chakraborty et al.	Optimization of biodiesel production using biological HAp as catalyst	4m ² /g	5.1 mmol HCl/g
12	2014	Chakraborty & RoyChowdhury	Methyl oleate synthesis optimization using Fe-HAp	14.9 m ² /g	10.336 mmol KOH/g
13	2015	Gao et al.	Gas phase dehydrogenation of ethanol using maleic anhydride as hydrogen acceptor using Cu-HAp as catalyst.	37 m ² /g	0.28 mmol NH ₃ /g
14	2015	Cai et al.	Synthesis and antimicrobial activity of mesoporous HAp-ZnO nanofibers.	24.81 m ² /g	-
15	2015	Buasri et al.	HAp catalyzed biodiesel production via microwave irradiation.	21.19 m ² /g	-

The above literature shows successful utilization of hydroxyapatite as a catalyst and catalyst support in various chemical reactions. The above observation has shown that HAp can be used as a cost effective catalyst and in many cases it has outperformed with respect to expensive metal oxide catalysts thus making the overall process cost effective. Therefore, in the present work, pork bone has been selected as raw material to develop hydroxyapatite (HAp) and has been employed in the esterification of glycerol with carboxylic acid.

3.1.5 Present Work: Literature Review

3.1.5.1 Diacetin and Triacetin Synthesis

Esterification of glycerol and acetic acid yields three products viz. monoacetin, diacetin and triacetin. Among these monoacetin is used in polymer industry and in cryogenic. Whereas diacetin and triacetin being the most important product of glycerol and acetic acid esterification are used as a fuel additive. Some other applications also include as plasticizer, solvent, softening agent and in cosmetic industry. Literature review shows that diacetin and triacetin can be used as a potential biodiesel additive to improve its property. Earlier reported work shows that no. of attempts have been made to maximize second degree and third degree ester. Although from [Table 3.1](#) it can be concluded that synthesis of diacetin & triacetin is quiet lengthy as it takes longer reaction time upto 3hr and higher reaction temperature upto 300°C which makes the process economically unfavorable. So in our present research work we have made an effort to produce diacetin & triacetin via esterification of glycerol and acetic acid in a shorter route. In the next section we will discuss about various application of antimony oxide catalyst which has been used as activating agent, wet impregnated on HAp support.

3.1.5.2 Antimony as Catalyst

Different types of supported antimony oxide Sb_2O_3 , Sb_2O_5 and Sb_2O_4 catalysts have been prepared to catalyze wide variety of chemical reactions. Among these oxides Sb_2O_3 is most important as a commercial compound. *Duh (2002)* have applied antimony catalyst (Sb_2O_3) for solid state polycondensation of poly ethylene terephthalate (PET). To study the effect of antimony catalyst (Sb_2O_3) on solid state polycondensation (SSP) antimony (Sb) concentration was varied between 0-210 ppm. It was observed that activation energy of the process decreased linearly when antimony (Sb) concentration lied between 0-100 ppm and the rate of solid state polycondensation (SSP) reached its maximum at antimony (Sb) concentration of 150 ppm. Activation energy for antimony catalyzed solid state polycondensation was found to be 23.3 kcal/mol at antimony (Sb) concentration of 210 ppm where as for uncatalyzed reaction it was 30.7 kcal/mol. However it was observed that upon increasing antimony (Sb) concentration frequency factor of the reaction decreased due to hindrance created by antimony molecules to heavier polymeric chain. Aluminum supported vanadium-antimony oxide catalyst ($\text{VSbO}_x/\text{Al}_2\text{O}_3$) has been employed in dehydrogenation of ethylbenzene with carbon dioxide and its effect was studied by *Park et al. (2003)*. A comparative study was made between catalytic activity of alumina supported vanadium oxides ($\text{VO}_x/\text{Al}_2\text{O}_3$) and vanadium-antimony oxides ($\text{VSbO}_x/\text{Al}_2\text{O}_3$). It was found that catalytic activity and on-stream stability of vanadium-antimony oxide ($\text{VSbO}_x/\text{Al}_2\text{O}_3$) catalyst was superior to vanadium-antimony oxide ($\text{VO}_x/\text{Al}_2\text{O}_3$) catalyst. The reason behind improved performance of $\text{VSbO}_x/\text{Al}_2\text{O}_3$ catalyst was addition of antimony into vanadium oxides ($\text{VO}_x/\text{Al}_2\text{O}_3$) which enhanced dispersion of active vanadium-oxide (VO_x) as well as redox property of system. *Zhang et al. (2004)* reported that very selective partial oxidation of methane (CH_4) to formaldehyde (HCHO) has been achieved using antimony oxides mainly Sb_2O_3 or Sb_2O_5 highly dispersed on silica. Different loading of antimony salt on silica has been reported. It has been found that antimony oxide (SbO_x)

loading up to a value of 20% in $\text{SbO}_x/\text{SiO}_2$ has demonstrated very good selectivity towards formaldehyde (HCHO) even at elevated temperature of 650°C . At this temperature $\text{Sb}_2\text{O}_5/\text{SiO}_2$ has been reported to be more selective with selectivity upto 41% towards formaldehyde than $\text{Sb}_2\text{O}_3/\text{SiO}_2$. *Mahajan et al. (2006)* has reported the application of hydroxylapatite (HAp) supported antimony catalyst (Sb-HAp) for stereo selective synthesis of trans-pyrano[3,2-c]quinolines from anilines, benzaldehydes and 3,4-dihydro-2H-pyran (DHP). It was found that the catalyst very efficient with good yield. The major advantage of the catalyst was its recoverability and it was reused ten times. *Zhang and Liu (2008)* found that antimony trichloride (SbCl_3) doped on silica gel ($\text{SbCl}_3/\text{SiO}_2$) acted as an efficient catalyst for the synthesis of 9-ary-3,4,5,6,7,9-hexahydroanthene-1,8-diones by condensation of aromatic aldehydes and 5,5-dimethyl-1,3-cyclohexanedione under solvent-free conditions. Application of developed catalyst ($\text{SbCl}_3/\text{SiO}_2$) resulted in shorter reaction time, higher yield, modest reaction condition, simple reaction set up and it also featured reusability. *Darabi et al. (2009)* reported that presence of lewis acid sites on antimony chloride (SbCl_3) doped silica catalyst ($\text{SbCl}_3/\text{SiO}_2$) performed very efficiently for the synthesis of quinoxaline derivatives even in the presence of low active substrate. Impregnation of antimony chloride (SbCl_3) on silica has appreciably increased the activity because of the formation of O–Sb–Cl bond which has facilitated as stable lewis acid site during the course of reaction. It was noted that the silica-antimony chloride catalyst ($\text{SbCl}_3/\text{SiO}_2$) showed long shelf life and excellent activity in reaction as well its preparation and handling was also user friendly. Even the catalyst was recovered and reused four times without any significant loss in its activity. The fact that SbCl_3 did not leach makes $\text{SbCl}_3/\text{SiO}_2$ as alternative heterogeneous acid catalyst to the conventional homogeneous acids at room temperature. *Pan et al. (2011)* developed antimony (Sb) impregnated tin oxide supported on carbon black (ATO/C) catalyst using precipitation method and further treated it with platinum (Pt-ATO/C) to enhance its catalytic activity for methanol oxidation. It was observed that Pt-

ATO/C catalyst showed a relatively higher activity towards methanol oxidation than commercial Pt/C catalyst (Pt-SnO₂/C). The reason behind higher activity was antimony (Sb) doping on tin oxide (SnO₂) and its electronic effects with Pt catalysts. Antimony-doped metal oxides as a co-catalyst of Pt, could be a promising and convenient methanol-oxidation anode catalyst. The above literature review has shown that antimony has been used as a catalyst in various chemical reactions and as a result it has enhanced the overall reaction performance. Therefore, in the present research work an attempt has been made to develop heterogeneous catalyst using antimony (Sb) on naturally derived hydroxylapatite (HAp) support and applied in glyceryl synthesis.

3.1.5.4 Optimization Study using Taguchi Design

Previously, process optimization had been conducted using classical method with large sets of experimental trials, but in recent time a power full statistical tool, Taguchi L₉ orthogonal matrix (TOLM) had been applied in various processes due to its advantages in providing sufficient information about the undergoing process utilizing minimum experimental trials and therefore enhancing process robustness (*Chowdhury et al., 2014, Kang et al., 2016*). *Nripjit et al. (2012)* has reported that Taguchi optimization offered process solution in most logical, economical, and statistical ways. In this method best possible performance is achieved by reducing number of experiments and a set of optimum experiments are generated using process factors which is called orthogonal array. The obtained results are analyzed and effect of process factors are studied by analyzing means and variance. Thus in the present work taguchi optimization a powerful statistical tool has been used to optimize the process.

3.2 Ethyl Hexyl Acetate as Fuel Additive

Branched esters are well known for its improvement in cold flow properties. However, branched alcohols have very low cetane number which may result in incomplete combustion (*Dunn et al., 2001*).

Furthermore, *Knothe et al. 2003* reported cetane numbers of certain branched esters which has desirable cetane number.

Table 3.5: Cetane Number of fatty esters (*Knothe et al., 2003*)

Alcohol	Acid				
	Palmitic	Palmitoleic	Stearic	Oleic	Linoleic
Methyl	85.9	51	101	59.3	38.2
Ethyl	93.1	nd	97.7	67.8	39.6
Propyl	85	nd	90.9	58.8	44
Butyl	91.9	nd	92.5	61.6	53.5
iso-Propyl	82.6	nd	96.5	86.6	nd
iso-Butyl	83.6	nd	99.3	59.6	nd
2-Butyl	84.8	nd	97.5	71.9	nd
2-Ethylhexyl	98.2	nd	115.5	88.2	nd

It has been observed from [Table 3.5](#) that 2-ethyl hexanol has promising cetane number. Therefore 2-ethyl hexanol derived acetic ester has been attempted as fuel additive that is expected to reduce pour point and has also expected to maintain the cetane number thus resulting desirable fuel characteristics.

2-ethyl hexyl acetate produced through esterification of acetic acid with 2-ethyl-hexanol is a clear, mobile liquid with a characteristic ester odor (*Lei et al. 2013*). 2-Ethylhexyl acetate is a hydrophobic yet comparatively polar high boiler with good solvent power for cellulose nitrate and many natural and synthetic resins. It is therefore useful in paint and coating formulations, e. g. for cellulose nitrate paints. Its properties can also be exploited in coatings for brushing on, dip-coating and spraying, and for stove enamels. The main purpose of adding 2-ethylhexyl acetate is to improve flow and film formation. The product is also a good coalescing aid for emulsion paints.

CHAPTER-4

AIMS AND OBJECTIVES

4. AIMS AND OBJECTIVES

The aims and objectives of the project are:

1. Preparation of supported metal catalyst derived from waste natural resources.
2. Characterization of developed solid acid catalyst.
3. Performance study of the solid acid catalyst in esterification reaction.
4. Application of electromagnetic radiation to intensify esterification reaction.
5. Optimization of the process using Taguchi Orthogonal Design.
6. Engine Emission and Engine Performance Study.

CHAPTER-5

MATERIAL AND METHODS

5. MATERIALS AND METHODS

5.1 Reagents and Materials

Pork bone collected from local slaughter house. Acetic acid glacial (> 99%), glycerol anhydrous (> 98%), 25% aqueous ammonia solution, KOH, oxalic acid extrapure, methanol, molecular sieves (water adsorbent) and antimony (III) chloride (> 98%) were procured from Merck, India and triacetin > 99% pure from Sigma Aldrich. All the chemicals used for this study are of analytical reagent grade.

5.2 Pork bone Processing

Pork bone, a municipal slaughter house waste was washed rigorously with hot distilled water to eliminate fleshy and proteinaceous material. Then the material was ground into fine powder (150 mesh) using laboratory crusher followed by ball milling to obtain pork bone derived hydroxyapatite (PHAp). The PHAp was processed for wet impregnation using antimony (III) chloride (SbCl_3) precursor in a 500ml three-neck glass flask which was equipped with a centrally fixed mechanical stirrer and two reflux condensers. The mixture was stirred at 700 rpm and 90°C for 4h followed by drying at 100°C and subsequent calcination at 500°C to develop Sb_PHAp catalyst. Variable precursor loadings of 20 wt. %, 30 wt. % and 40 wt. % were used to prepare Sb_PHAp catalysts and designated as SH 2, SH 3 and SH 4 respectively.

5.3 Experimental Design

The independent factors and their levels had been scrutinized in a L_9 orthogonal array using Taguchi design. A standard Taguchi orthogonal L_9 matrix (TOLM) was used to execute the experiments in triplicates using three levels of the four process parameters viz., AA:G molar ratio (a_{MR}), Sb precursor loading (a_{CL}), catalyst concentration (a_{CC}) and reaction temperature (a_T) in AA-G esterification. The TOLM was applied to understand the parametric effects and to determine a set of optimal process

parameters corresponding to maximum combined yield (Eq. 1) of diacetin and triacetin (Y_{DT}) through SN ratios (Eq. 2) and analysis of variance (ANOVA) using MINITAB-16 (Minitab Inc. USA for Windows7) software. The nine experimental conditions are tabulated in Table 5.1 with corresponding yields and SN ratio.

$$Y_{DT} = \frac{\text{moles of (diacetin + triacetin) formed}}{\text{moles of G consumed}} \times 100 \quad (1)$$

$$S/N = -10 \log \left(\frac{1}{n} \sum_{i=1}^n \frac{1}{Y_{DT,i}^2} \right) \quad (2)$$

Where, i denotes number of replications, n implies number of trial experiments executed in a particular parametric set values as elaborated in Table 5.1.

Table 5.1: TOLM at different parametric conditions showing corresponding DT yield (Y_{DT}) and SN ratios.

a_{MR}	a_{CL} (wt. %)	a_{CC} (wt. %)	a_T (°C)	Y_{DT} (%)	SN Ratio (dB)
2:1	20	3	90	66±0.2	36.39
2:1	30	4	100	80.26±0.5	38.06
2:1	40	5	110	84±0.5	38.59
4:1	20	4	110	86.4±0.5	38.93
4:1	30	5	90	80.8±0.1	38.15
4:1	40	3	100	82±0.4	38.38
6:1	20	5	100	86.1±0.6	38.79
6:1	30	3	110	85.11±0.5	38.70
6:1	40	4	90	86.8±0.1	38.99

5.4 Catalyst Characterization

Structural features of pork bone supported Sb_PHA_p catalyst was evaluated using FTIR (Shimadzu (alpha) from 400 to 4000 cm⁻¹) analysis. Crystalline phases were identified by X-ray diffraction (XRD) using Rigaku Miniflex (Co., Japan) with Cu K α source with an Inel CPS 120 hemispherical detector. The scanning was done at 2 θ ranging from 10° to 90° at a speed of 1 min⁻¹. The specific surface area (SSA) and pore size distribution of the generated catalyst sample was measured by BET and BJH methods (Quantachrome make NOVA 4000e). Furthermore, effect of calcination temperature on PHA_p and dried Sb_PHA_p had been evaluated using Perkin–Elmer TGA analyzer (Pyris Diamond TG/DTA) in a platinum crucible under nitrogen atmosphere (150 mL/min) from 30 to 500°C. The morphology of wet impregnated and calcined Sb_PHA_p prepared at optimal precursor loading (determined by TOLM, [Table 5.1](#)) were studied by a Scanning Electron Microscope (SEM) at 17 KV (JEOL Ltd., Japan, model JSM 6700F).

5.5 AA-G esterification using Sb_PHA_p catalyst

The performance of the developed Sb_PHA_p catalyst was evaluated through AA-G esterification over a fixed reaction time of 2h in a three-neck glass flask (capacity: 250 mL) fitted with a centrally placed mechanical stirrer, a digital speed regulator (REMI, RQ-121/D, AXIAL TURBINE) and two reflux condensers holding measured amount of molecular sieves were attached to the other two necks. IR radiation (150W; far infrared wavelength: 2700–30,000 μ m) was employed to expedite the ester yield. To determine the time required to achieve similar DT yield as in case of IRI, experiments were performed at TOLM derived optimized parametric combination, in a conventionally heated (300 W) batch reactor (CHBR) and was compared with infrared radiation aided batch reactor (IRRABR) in terms of energy efficiency.

Furthermore, after completion of each reaction, the reaction mixture was cooled and vacuum filtered to separate catalyst and subsequently the filtrate was subjected to vacuum drying to remove traces of water before GC-MS analysis. The ester obtained was analysed using GC-MS (Agilent 7890 gas chromatograph coupled with HRMS Jeol, Accu TOF GCV) with HP5 capillary column (30 m length, 0.32 mm i.d., 0.25 μm film thickness). The temperature program was as follows: 40 $^{\circ}\text{C}$ for 2 min, 10 $^{\circ}\text{C}/\text{min}$ up to 250 $^{\circ}\text{C}$. Furthermore, following equations were used to determine G conversion and desired product selectivity using GC-MS data points.

$$\text{G Conversion (\%)} = \left(\frac{\text{Moles of G consumed}}{\text{Moles of G initially taken}} \right) \times 100 \quad (3)$$

$$\text{Product Selectivity} = \left(\frac{\text{Moles of desired product formed}}{\text{Total product moles}} \right) \times 100 \quad (4)$$

5.6 Reusability protocols for catalyst

The recovered catalyst was subsequently washed with methanol and oven dried at 105 $^{\circ}\text{C}$ and then reused for next catalytic run to estimate its reusability characteristics.

5.7 Engine Performance Test

Single cylinder four stroke standard diesel engine (Engine Specifications, Make: Kirloskar AV-1, Rated Power: 3.7 kW, 1500 rpm, Compression Ratio: 16.5:1 and variable from 13 to 20 (approx.), Cylinder Capacity: 553 cc) had been used to evaluate the performance of experimentally synthesized product (ESP) blended with palm biodiesel (B100). Engine was operated with varying engine speed of 1400-1600 rpm. Engine runs had been conducted with B 100 and DT blends (3 vol. % – 7 vol. %) and compared with commercial triacetin using identical blend proportions. Emission analysis had been executed using exhaust gas analyzer having following measurement range: CO: 0–15%; HC: 0–20,000 ppm; CO₂: 0–20%; NO_x: 0–5,000 ppm.

CHAPTER-6

RESULT AND DISCUSSION

6. RESULTS & DISCUSSION

6.1 Glycerol acetic acid esterification with pork bone supported antimony HAp catalyst

6.1.1 ANOVA Study and Optimal Condition Evaluation

ANOVA analysis has been elaborated in [Table 6.1](#) where it can be well identified that AA:G mole ratio and reaction temperature having p-value ≤ 0.05 are the most significant factors affecting Y_{DT} (Eq. 1).

Whereas, catalyst concentration and Sb precursor loading having p-value > 0.05 affect Y_{DT} insignificantly.

Table 6.1: Analysis of variance for DT Yield.

Source	DF	Seq. SS	Adj. SS	Adj. MS	F	p	Values
AA:G (a_{MR})	1	161.31	161.31	161.31	13	0.023	
Sb precursor loading (a_{CL})	1	40.56	40.56	40.56	3.27	0.14	
Catalyst Concentration (a_{CC})	1	52.16	52.16	52.16	4.2	0.10	
Reaction Temperature(a_T)	1	93.69	93.69	93.69	7.55	0.05	
Error	4	49.64	49.64	12.41			
Total	8	397.35					
R^2							0.90

Additionally, F-values ([Table 6.1](#)) and Δ -values ([Table 6.2](#)) also evidence the significance of the process factor over Y_{DT} . Therefore, the comparative effects can be represented in the order $a_{MR} \succ a_T \succ a_{CC} \succ a_{CL}$ which has also been well elaborated in [Table 6.2](#) depicting optimum values at the respective levels of AA:G (Level 3), Sb precursor Loading (Level 3), catalyst concentration (Level 2) and reaction temperature (Level 3) corresponding to achieve maximum Y_{DT} .

Table 6.2: Response Table for Signal to Noise (SN) ratio.

Level	a_{MR}	a_{CL}	a_{CC}	a_T
1	37.68	38.04	37.82	37.84
2	38.49	38.30	38.66	38.41
3	38.83	38.65	38.51	38.74
Delta	1.15	0.62	0.84	0.9
Rank	1	4	3	2

Fig. 6.1 describes the individual effect of parameters (in terms of SN ratios) on Y_{DT} , which has also been validated and explicated by taking individual experimental trials while setting the other operating parameters at their optimum

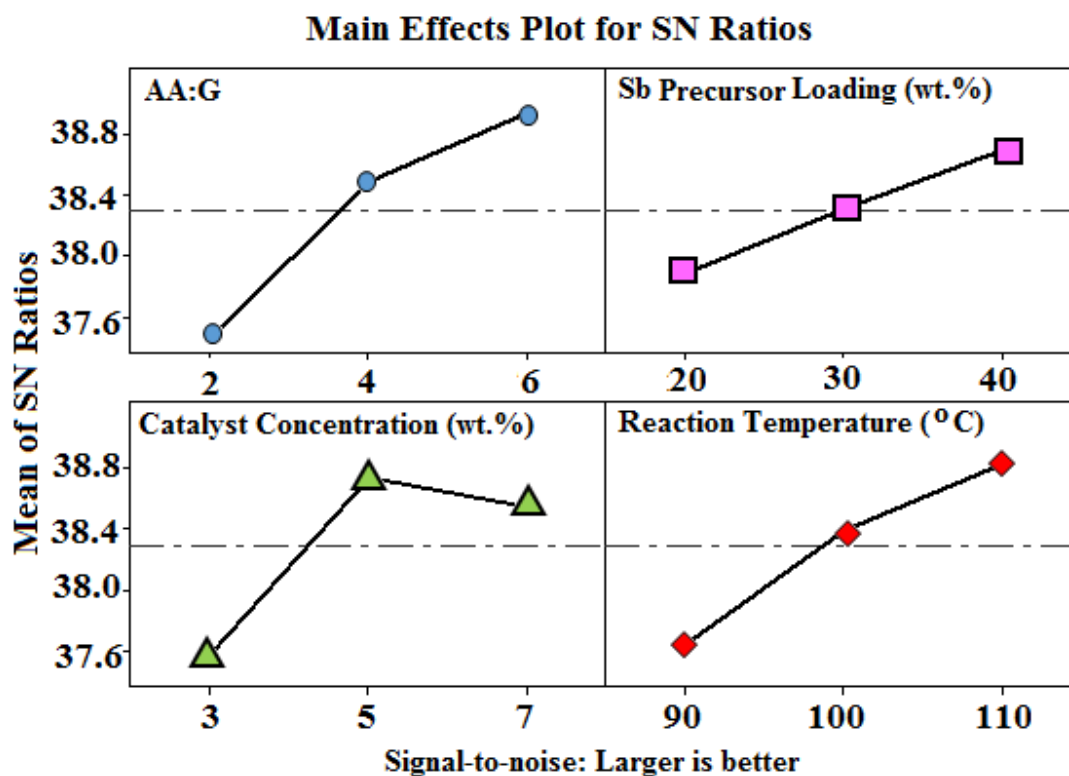


Fig. 6.1 Individual Plot representing parametric effects.

6.1.2 Contour plot

Contour plots were analyzed to visualize the effect of the factors on responses. Overlay contour plots describing the effect of significantly contributing factors. Effect of reaction parameters on DT yield has been represented in Fig. 6.2 using contour plot. In the figure area of DT yield has been discretized in different color shades, the region of dark green color represents the highest response and a region of dark blue color represents lowest response. From the figure it is quite clear that combined effects of mole ratio and temperature have resulted in maximum DT yield of more than 90% followed by precursor loading and catalyst concentration. Whereas, other interactive parameters show more or less similar significance on DT yield. Overall, from the contour plot it can be concluded that all the operating parameters have synergistic effect on DT yield. Furthermore, it is worthwhile to mention here that the obtained experimental values are regressed with linear model to reduce the complexity of the present system.

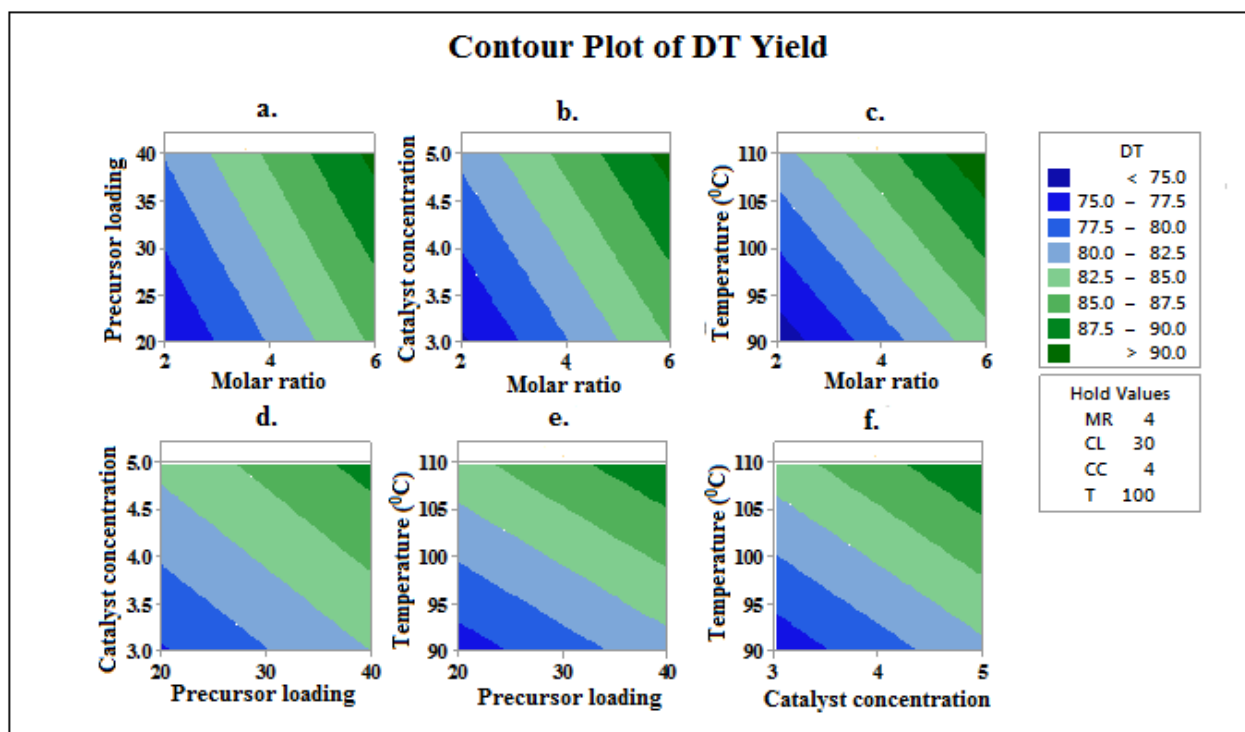


Fig. 6.2 Contour Plot showing parameter interaction & DT yield

6.1.3 Effect of Process Parameters on DT Yield

6.1.3.1 Effect of AA:G Mole Ratio

Influence of AA:G mole ratio was found maximum on DT yield. AA:G mole ratio has been varied between 2:1 to 8:1 to maximize DT yield, while other parameters has been fixed at their optimum levels. It was observed that increase in AA:G could enhance the G conversion (Eq. 3) due to excess of AA in the reaction system (*Ferreira et al.,2009*) ; however further increase above 6:1 ratio resulted minimal change in G conversion and least alteration in DT yield (*Liao et al.,2009*).

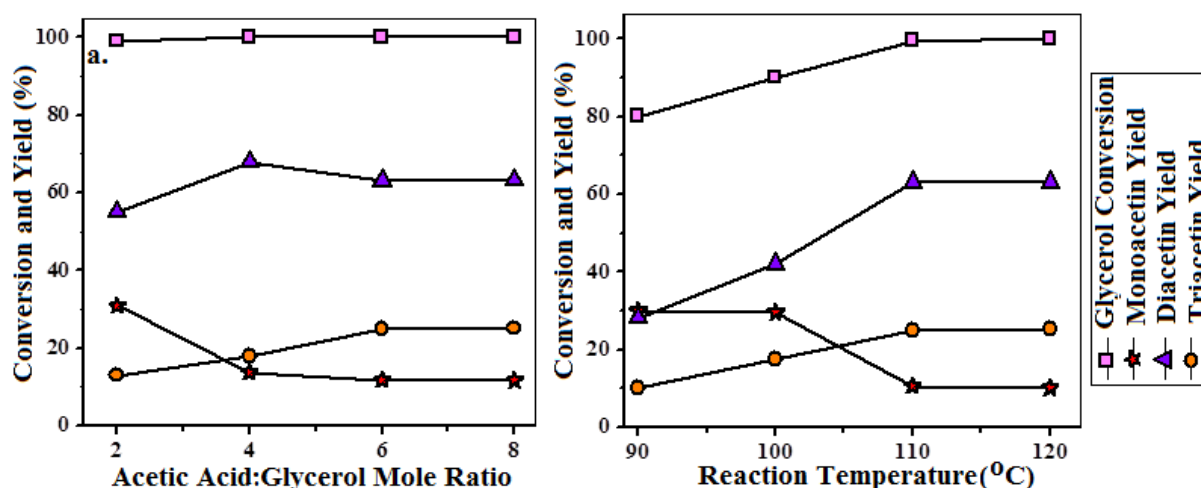


Fig. 6.3 Effect of a. AA:G mole ratio and b. Reaction Temperature on G conversion and ester yield (at optimal condition).

6.1.3.2 Effect of Temperature

Reaction temperature in case of IRRABR has been varied between 90 - 120°C to estimate the conversion of G and yield of monoacetin, diacetin and triacetin while maintaining other parameters at their optimum values. It can be well depicted from Fig 6.3b that increase in temperature results in higher G conversion (*Hasan et al.,2015*) from 80±1% - 99±1% and attains maximum at 110°C which corroborates well with findings of (*Rodriguez et al.,2011*). It has also been observed, that at lower temperature, monoacetin availability was preponderant and as the temperature increased DT yield has

increased in expense of monoacetin yield (*Liu et al.,2011*) where water formed being adsorbed in molecular sieves. Successively, excess AA reacts with monoacetin and diacetin and forms triacetin. Therefore, to maximize DT yield, optimum reaction temperature was selected at 110°C which substantiates the selection of process parameters for Taguchi prediction.

6.1.3.3 Effect of Catalyst Concentration

As exhibited in [Fig. 6.4a](#) increase in catalyst concentration from 2 to 4 wt. % has resulted increase in G conversion from 90±0.5% to 99±1% corresponding to 20% increase DT yield due to availability of more active sites of the catalyst (*Balaraju et al.,2010*), while further increase has an antagonistic effect which may be due to the mass transfer hindrance created by excess amount of catalyst for a fixed volume of reactor.

6.1.3.4 Effect of Sb precursor loading

[Fig. 6.4b](#) depicts increase in Sb precursor loading from 20 to 40 wt. % results 4±0.6% more increase in G conversion with 6±1% more increase in DT yield. This can be correlated to the fact that increase in Sb precursor loading results in increase in Lewis and Bronsted acidic sites of Sb_PHA_p catalyst promoting more nucleophilic attack of the hydroxyl group of monoacetin with AA adsorbed on the catalyst surface, thus ensuing more conversion of monoacetin to diacetin and triacetin.

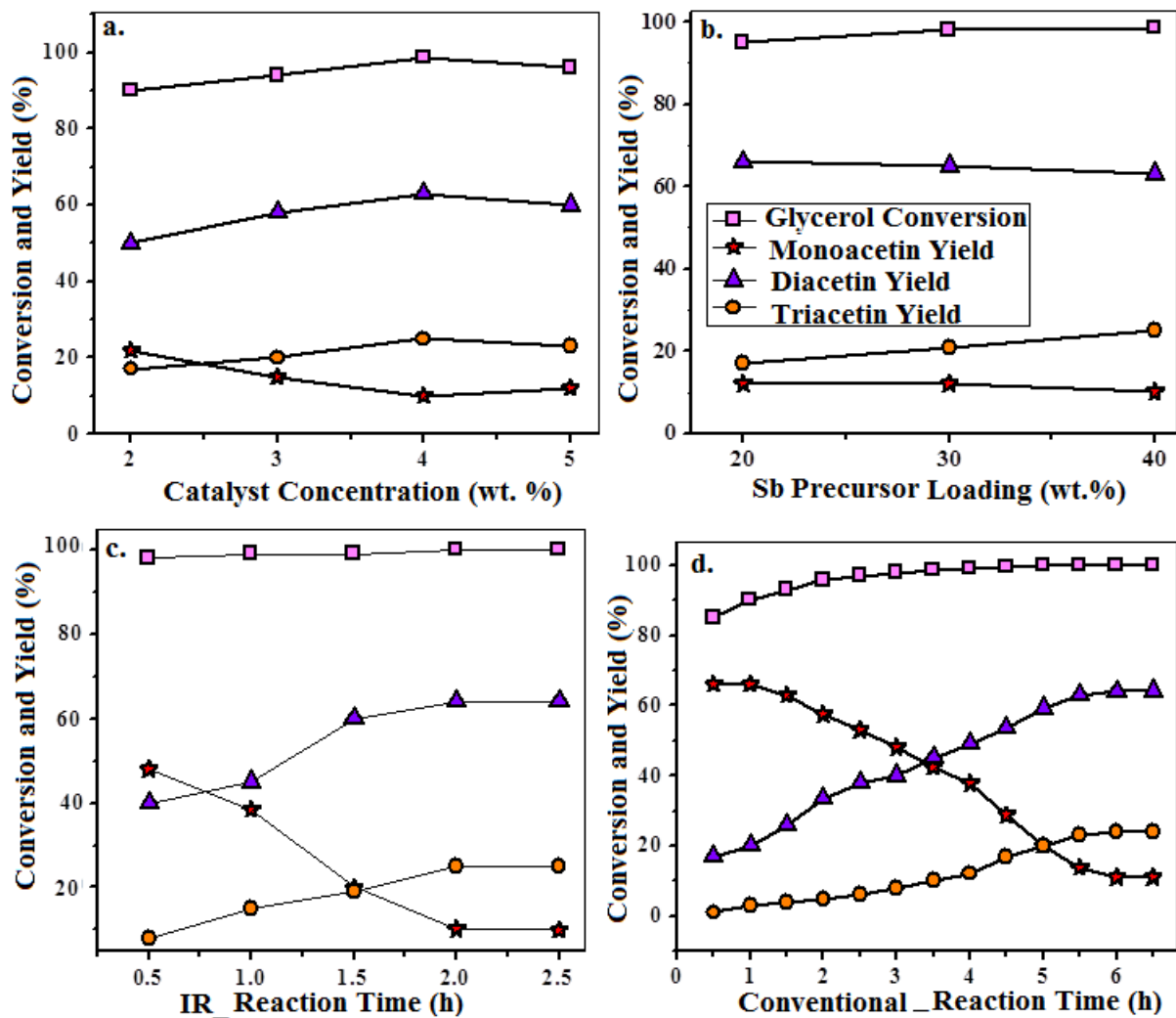


Fig 6.4. Effect of a. catalyst concentration, b. Sb precursor loading, Reaction time c. for IRRABR and d. for CHBR on glycerol conversion, diacetin and triacetin yield.

6.1.3.5 Effects of Reaction Time

Under optimal parametric condition, it has been observed that increase in reaction time resulted consistent G conversion with increase in DT yield from $60 \pm 1\%$ obtained at 1h to $88 \pm 1\%$ at 2h and remained more or less constant with further increase in reaction time as depicted in Fig. 6.4c. Furthermore, in comparison with Fig. 6.4d, 6.4c also exemplifies the energy efficacy of IRI over CH, consuming lesser reaction time for maximum DT yield. For $88 \pm 1\%$ DT yield, IRRABR consumed 2h at

the energy input rate of 150 J/s whereas, CHBR consumed 6h at the energy rate of 300 J/s. This implies, that to achieve maximum DT yield at derived optimal condition CHBR consumed 6 folds higher energy input compared IRRABR.

6.1.3.6 Effects of IR Activation at optimal condition

It has been established that polar molecules generally absorb electromagnetic radiation and get excited from its ground state to vibrational state; thus, creating intense molecular collision promoting chemical reaction (*Chakraborty et al.,2015*). It can be observed from [Table 6.3](#) that, IR activation has profoundly increased the DT selectivity compared to conventional heating. This phenomena advocates the fact that the thermal energy generated in case of IR activation promotes much faster stimulation of reactive species; thus, enabling quick conversion of monoacetin into diacetin and triacetin. Even, in case of a blank run, it has been observed that IR activation resulted 13% more G conversion with 36.3% yield towards DT compared to conventional heating with only 10.3% DT yield under optimal condition.

Table 6.3: Effect of IR activation and different catalysts on DT selectivity (Eq. 4).

Activation Mode	Catalyst Used	G Conversion (%)	Yield (%)		
			Monoacetin	Diacetin	Triacetin
IR	Blank	80±0.8	43.1	28	8.3
	SH 4	99±1	10.4	63.6	25
	Amberlyst 15	99±1	7	66	26.8
Conventional Heating	Blank	67±0.6	56.1	10	0.3
	SH 4	95.8±1	57.4	33.43	4.8

Evidently, from [Table 6.3](#), it can also be inferred, that the prepared SH 4 catalyst demonstrated performance close to commercial Amberlyst 15 under similar operating condition; this advocates the high efficacy of the prepared low cost catalyst.

6.1.4 Catalyst Characterization

6.1.4.1 TGA Analysis

Thermo-gravimetric analysis (TGA) pictogram (Fig. 6.5) demonstrates the weight loss of PHAp and uncalcined SH 4 samples over heating range of 30-500°C. TGA indicates 27.55% and 33.24 % major weight loss from PHAp and SH 4 samples respectively due to evaporation of absorbed water. Further weight loss of 7.88% from PHAp and 4.23% from SH 4 samples were also observed depicting water loss from lattice surface owing to disintegration of macromolecules and other organic substances.

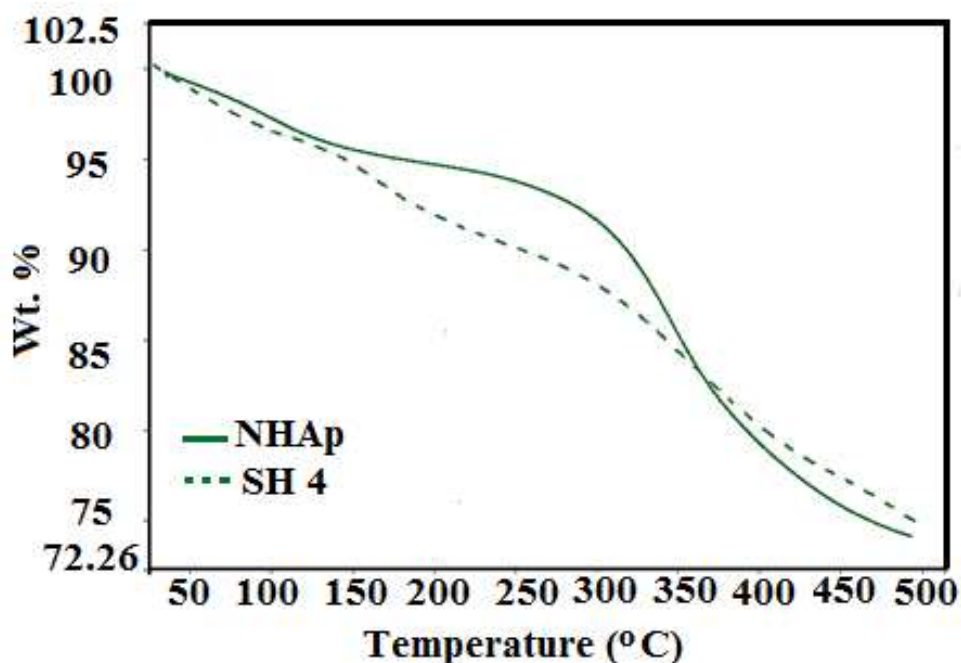


Fig. 6.5. TGA Analyses of NHAp and SH 4 samples.

On additional heating between 300-500°C, 19.1% weight loss from PHAp and 12.5% weight loss from SH 4 can be correlated to solid state reaction corresponding to the formation of gaseous elements and transformation of SbCl_3 to Sb_2O_5 (Yang *et al.*,2012) in PHAp and SH 4 respectively. No β - tricalcium phosphate has been formed at 500°C (Kupiec & Wzorek,2012) in PHAp and SH 4 (confirmed in XRD analyses). Since PHAp and SH 4 exhibited stable nature up to 500°C; hence, presence of all probable crystalline phases could be expected upon calcination at this temperature.

6.1.4.2 FTIR Analysis

The FTIR result corresponding to SH 2, SH 3 and SH 4 catalyst are shown in Fig. 6.6. The FTIR peak corresponding to 3404 cm^{-1} represents OH^- vibration (Chakraborty & RoyChowdhury,2014) whereas, peak at 1634 cm^{-1} denote bending mode of OH group. The bending mode at 2340 cm^{-1} and 1538 cm^{-1} denotes O-C-O stretching. The bands at 1450 cm^{-1} and 1400 cm^{-1} represent carbonyl group (Sanosh et al.,2009). FTIR wave number 2082 cm^{-1} and 1995 cm^{-1} represent CO^{3-} stretching vibration. Notably, the broad peak located at 740 cm^{-1} correspond to the presence of Sb_2O_5 (Miller et al.,1952). Additionally, the peaks at 1050 cm^{-1} , 608 cm^{-1} and 560 cm^{-1} characterize vibration of PO_4^{3-} group (Rehman et al.,1997).

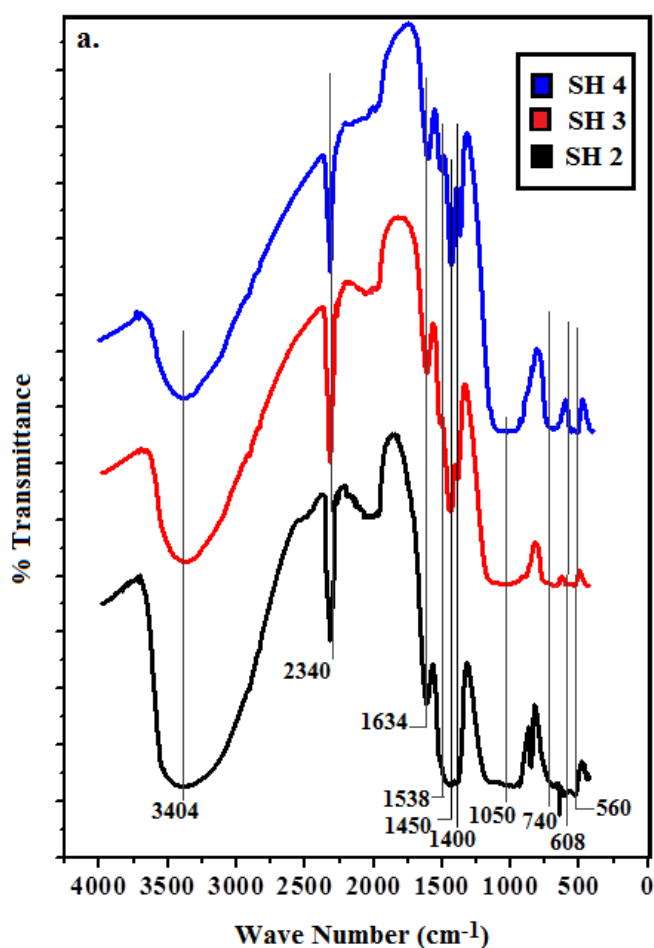


Fig. 6.6. FTIR analyses of Sb_PHA catalyst.

6.1.4.3 XRD Analysis

XRD patterns of the prepared catalyst obtained at three different precursor loadings (SH 2, SH 3 and SH 4) are illustrated in Fig. 6.7. Different crystalline phases present in the catalyst sample has been identified and compared using standard JCPDS card numbers 32-0044 and 33-0111 for antimony oxide and 89-4405 for PHAp. From Fig. 6.7, it can be well identified that SH 4 and SH 3 possess prominent cubic phase of $\text{Sb}_2\text{O}_5 \cdot 4\text{H}_2\text{O}$. On the other side, SH 2 catalyst samples depicts very low intensity $\text{Sb}_2\text{O}_5 \cdot 4\text{H}_2\text{O}$ peaks. Thus, increase in Sb precursor load could amplify the peak intensity along with narrowing of peak width (*Xiong et al., 2003*). Furthermore, monoclinic HAp phases are also observed in all catalyst samples, whereas, high intensity HAp phases have been detected in SH 2 catalyst compared to catalysts having high Sb precursor loading. This can be well credited to the fact that increase in Sb precursor doping could suppress HAp peaks in SH 4 and SH 3 catalyst samples. Interestingly, very low intensity Sb_6O_{13} phases are also noticed in SH 4 and SH 3 whereas, no such peaks have been observed in SH 2.

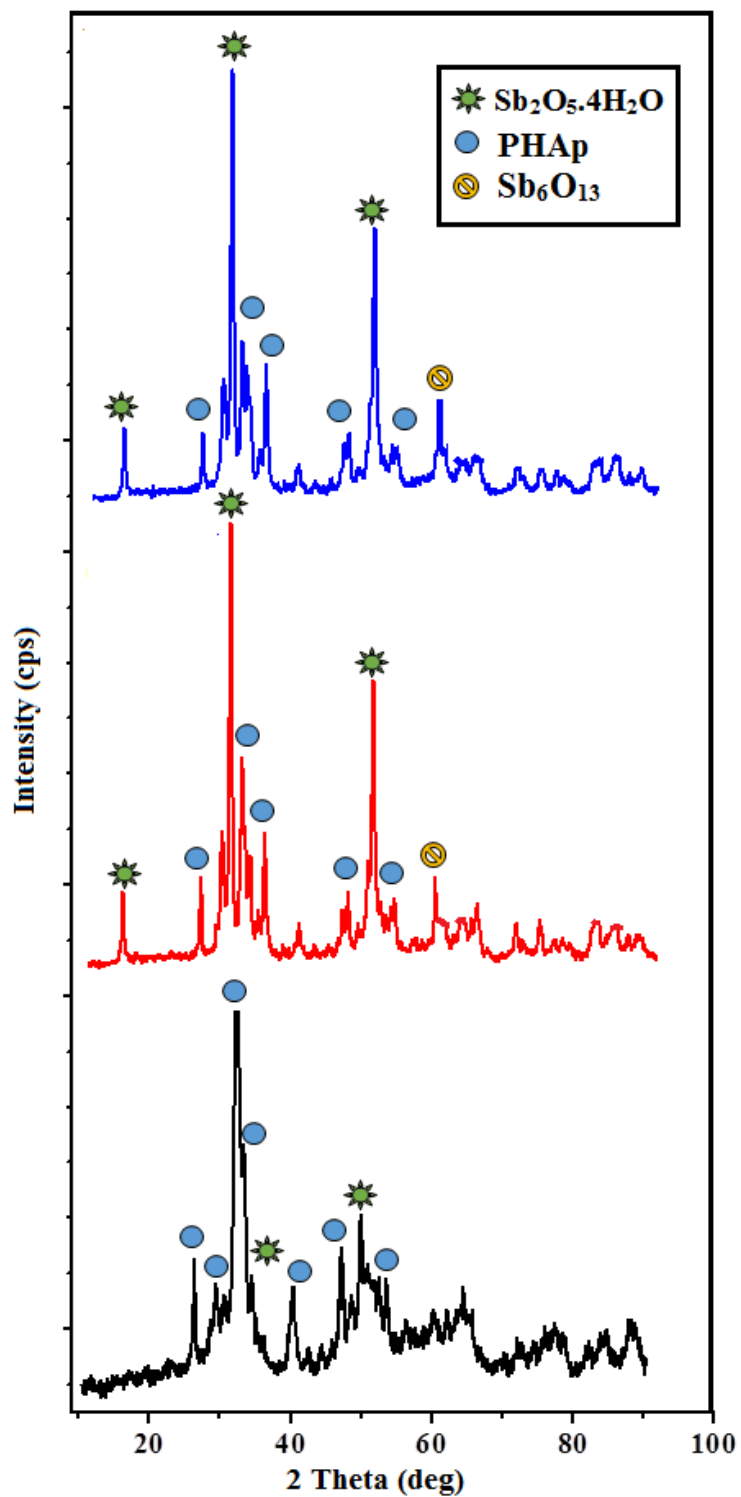


Fig. 6.7. XRD analyses of Sb_PHAp catalyst.

6.1.4.4 BET Analysis

Table 6.4 illustrates BET surface area of Sb_PHap catalysts (SH 2, SH 3 and SH 4). It has been clearly portrayed that increase in Sb precursor loading in SH4 has increased the SSA of the catalyst by nearly 50% (*Park et al.,2003*) with 4.5 nm average pore diameter. This has facilitated more G conversion and DT selectivity within shorter reaction time (2h). Moreover, all the catalysts exhibited appreciable pore volume with higher percentage of total pore volume being occupied by mesopores; this facilitates easy transport of reactants (molecular length of AA: 0.22 nm and G: 0.435 nm) without any steric hindrance (*Konwar et al.,2015*), thus promoting higher G conversion.

Table 6.4: BET Surface Area and Product Distribution.

Catalyst	SSA m ² /g	Total Pore Volume (cc/g)	Pore Nature			G Conversion (%)	DT Yield (%)	DT Selectivity (%)
			Microporous (%)	Mesoporous (%)	Macroporous (%)			
SH 2	12	0.017	58.7	41.22	-	95	82	86
SH 3	19.61	0.041	25.2	64.81	10	97.5	86	87
SH 4	40.02	0.0485	8.25	78	13.32	99.6	89	89.8

6.1.4.5 SEM Analysis

Microscopic analysis of dried and calcined SH 4 catalyst has been depicted in Fig. 6.8a and 6.8b respectively. Before calcination, the morphology of the catalyst shows uneven distribution of non-agglomerated granules over porous PHAp. Whereas, on calcination, agglomeration of particles occurs with irregular distribution of pores over smooth catalyst support surface.

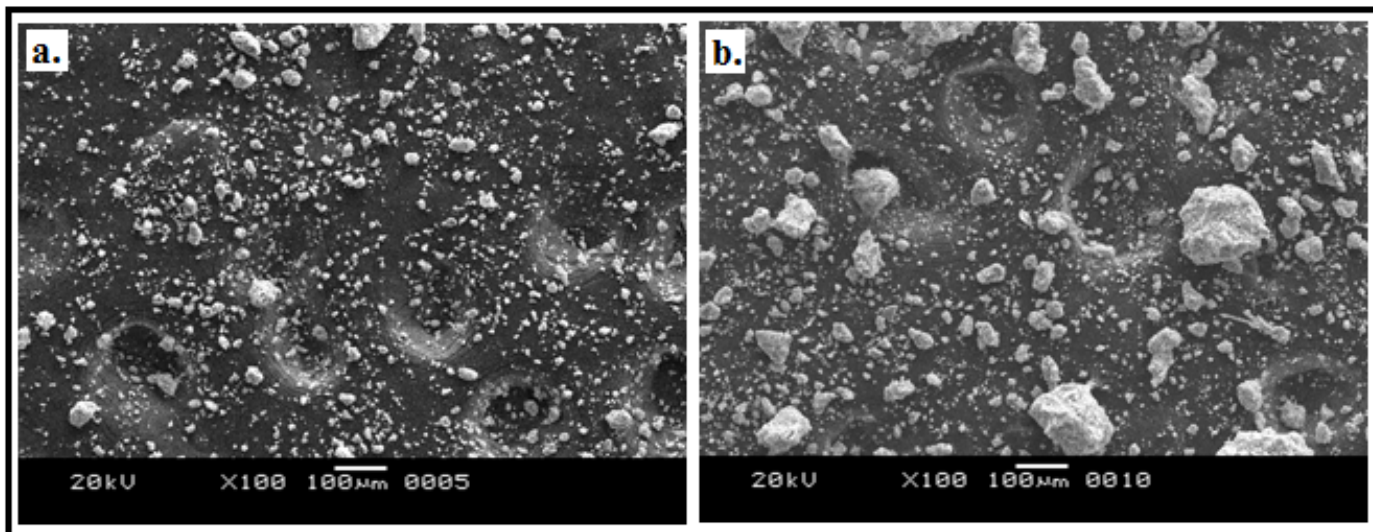


Fig. 6.8. SEM Micrograph of a. dried SH 4 and b. calcined SH 4.

6.1.4.6 Catalyst Recycling

Efficacy of heterogeneous catalyst depends on its uninterrupted reusability in experimental cycles. The SH 4 catalyst showing maximum G conversion and DT yield was separated by vacuum filtration after each reaction cycle and washed thoroughly with methanol until no reactant traces were left. Subsequently, it was subjected to oven drying until it was completely dry and then used for next experimental trial. Fig. 6.9 enumerates that the developed catalyst could be reused for eight successive experimental cycles giving $99\pm 1\%$ G conversion consistently and after that there was a slight drop in G conversion which may depict its loss in catalytic activity.

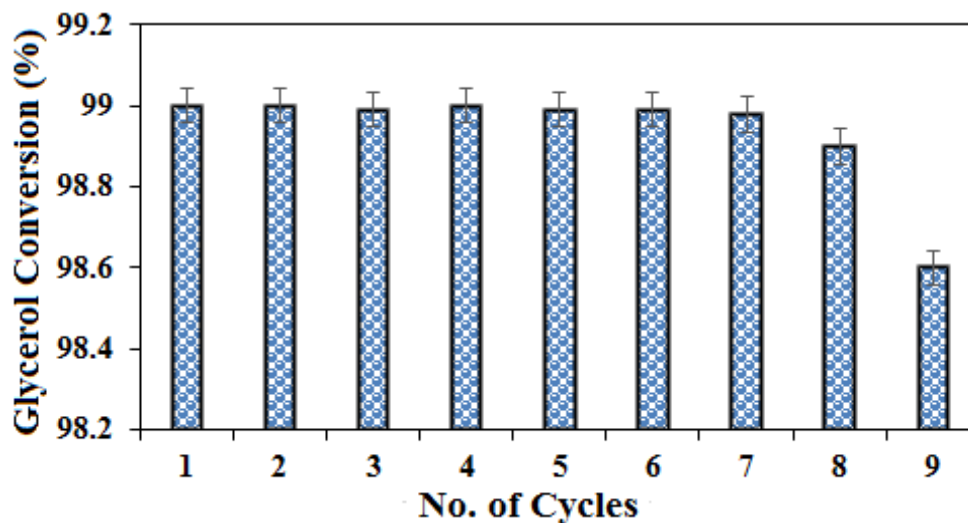


Fig. 6.9. SH 4 catalyst reusability in esterification of G with AA.

6.1.5 Probable Reaction Mechanism

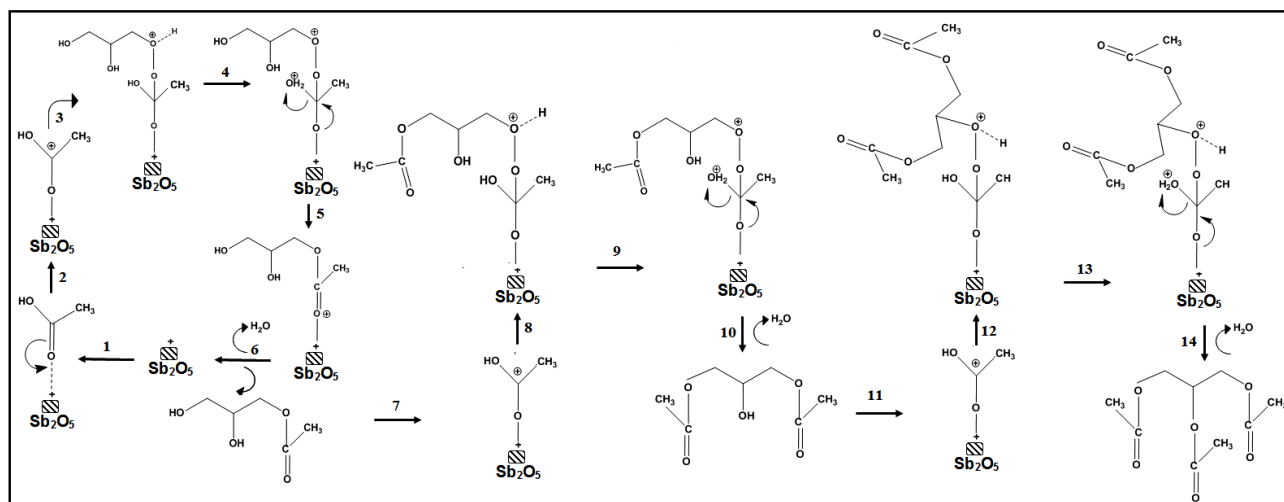


Fig. 6.10. Probable Reaction Mechanism for esterification of G with AA.

Fig. 6.10 illuminates, AA undergoes a nucleophilic attack with the Lewis acidic site of SH 4 catalyst (Step 1). This attack results in protonation of the carbonyl group present in the AA (Step 2), thus acquiring a positive charge (*Ferreira et al.,2009*). Successively, the carbonyl atom gets attacked by the OH group of G resulting an intermediate (Step 3) with C-O bond (Step 4, 5) (*Sun et al.,2016*). Water gets eliminated due to transfer of charges and gets adsorbed on the molecular sieves along with

generation of monoacetin (Step 6). Since, no steric hindrance present in the catalyst (evidenced from pore volume of SH 4), therefore, only 1-monoacetin has been detected in the product. Subsequently, formed 1-monoacetin reacts with the carbonyl group of AA (Step 7, 8, 9) that has already been attached to the catalyst surface yielding diacetin (Step 10). The diacetin consecutively undergoes further esterification reaction with the excess acid present in the system (Step 11, 12, 13) and finally renders triacetin (Step 14) (*Zhu et al.,2013*).

6.1.6 Fuel Property Evaluation

[Table 6.5](#) enunciates the addition effect of the experimentally synthesized product (ESP) (containing $88\pm 1\%$ DT) on fuel properties of palm biodiesel (B100) and its comparison with commercial triacetin (CT). The additives have been added in varying proportions from 3 - 7 vol. % and designated as BP3, BP5 and BP7 for ESP and BC3, BC5 and BC7 for CT respectively. It is worthy to mention here, that according to EN 14214 standard, triacetin vol. % in biodiesel should not exceed 7.7 vol. %; hence, in this study the blends have been kept within the suggested range (*Casas et al.,2010*). [Table 6](#) indicates that after addition of both the synthesized product and commercial product, all the fuel properties could strictly follow the EN standards. Notably, increase in both ESP and CT proportions has improved the pour point of B100 which in compliance with the study of (*Garci'a et al.,2008*) . However, its further addition has been restricted; since, it lowers flash point and cetane number. Therefore, [Table 7](#) illustrates the fact that the ESP demonstrated comparable results with CT.

Table 6.5: Effect of commercial Triacetin and Experimental Product application on Palm Biodiesel.

Properties	Palm Biodiesel (B 100)	BP3	BP5	BP7	BC3	BC5	BC7	EN
								14214 2008
Density g/cc	0.875	0.876	0.88	0.889	0.878	0.885	0.89	0.86- 0.90
Viscosity mm ² /s at 40°C	4.482	4.49	4.492	4.496	4.483	4.486	4.49	3.5-5.0
Flash Point, °C	164	150	135	125	156	155	143	101 min
Acid No. mgKOH/g	0.31	0.38	0.40	0.45	0.32	0.33	0.355	0.5 max
Cetane No	64.1	60	58	56.3	62	59.1	58	≥ 51
Cloud Point, °C	17	16.2	15.8	15.0	16.0	15.5	14.9	Report
Pour Point, °C	15	15.1	14.0	13.0	14.5	13.2	12.5	Report

6.1.7 Engine Characteristics

6.1.7.1 Engine Emission

Figure 6.11 represents emission values obtained for different test fuels operated at engine speeds 1400-1650 rpm. As observed from Fig. 6.11a, that increase in vol. % of both CT and the ESP, resulted almost 50% decrease in CO emission; thus exhibiting more complete combustion. This has resulted due to presence of higher oxygen in the blended fuels (*Kalam & Masjuki,2008*). Additionally, slight increase in CO₂ emission (Fig. 6.11b) has been detected on addition of CT and ESP (*Lacerda et al.,2015*). Whereas, Fig. 6.11c represents the data points for NO_x emission, it reveals that addition of both ESP and CT subtly affected NO_x emission by only 2%, which may be related to the slightly slower burning rate of the blended fuels due to comparatively lower cetane value than B100. Furthermore, almost 20%

reduction in HC emission has also been recorded for both ESP and CT, this may be ascribed to the higher oxygen content of the blended fuel; thus depicting cleaner burning of fuel.

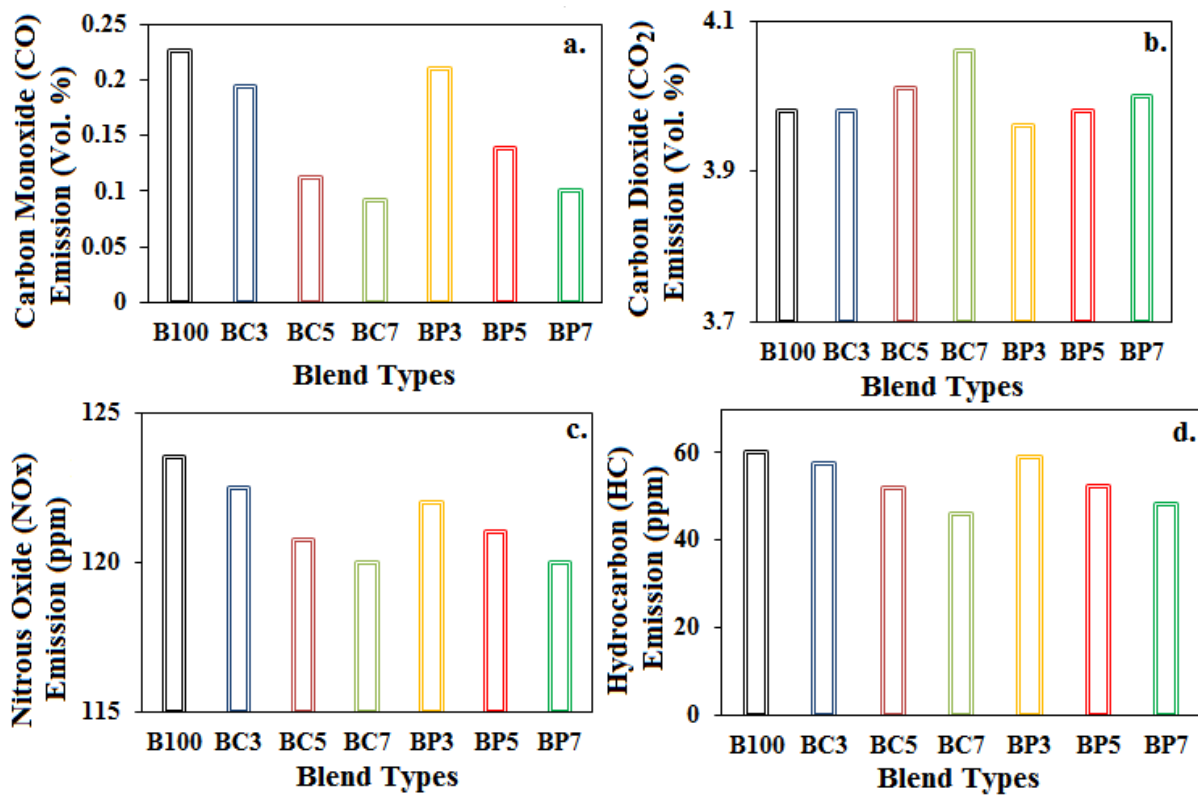


Fig. 6.11. Engine emission values for different test fuels.

6.1.7.2 Variation of engine emission with engine speed

6.1.7.2.1 Carbon monoxide (CO) emission

The CO emission for six different blend and neat biodiesel is represented in Fig. 6.12a. CO being an intermediate combustion product resulted from incomplete combustion of fuel. On complete combustion it is converted to CO₂. And the reason is shortage of air or low gas temperature which leads to incomplete combustion (Adaileh *et al.*, 2012). The present experimental study shows CO emission value lies in between 0.03-0.32 vol% and with increase in engine speed CO emission decreases in the tested engine speed range except for neat biodiesel which shows a decreasing trend upto 1500 rpm and then it increases. The decrease in CO emission is expected due to availability of higher oxygen in biodiesel and

triacetin which result in complete combustion. This explanation is in compliance with the research by *Kalam & Masjuki (2008)* and *Lapuerta & Armas (2008)*.

6.1.7.2.2 Carbon dioxide (CO₂) emission

The CO₂ emission for neat biodiesel and six biodiesel blend with additive is shown in *Fig. 6.12b*. The observation shows that CO₂ emission value lies in between 2.25-5.45 vol% and CO₂ emission decreases with increase in engine speed for all biodiesel blend and neat biodiesel. The trend shows that addition of additive increases CO₂ emission which shows availability of more oxygen (O₂) for complete combustion (*Oprescu et al., 2014*). The CO₂ emission from neat biodiesel is lowest compared to all other biodiesel blends. This can be attributed to higher CO emission as exemplified in *Fig. 11a*.

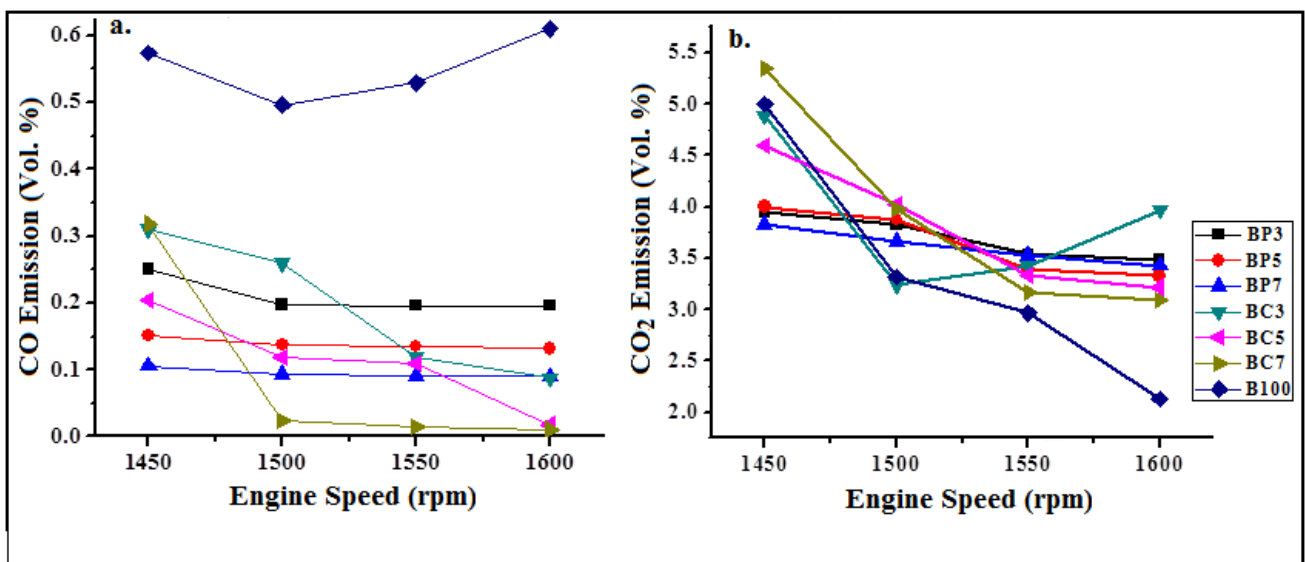


Fig. 6.12. Exhaust emission characteristics for palm biodiesel based diesel engine at different speed for a. CO b. CO₂

6.1.7.2.3 Hydrocarbon (HC) Emission

Hydrocarbon emission (HC) for six different biodiesel blends and neat biodiesel is represented in *Fig. 6.13a*. The HC emission value lies in the range of 52.5-72.5 ppm for all the blends. From the figure it can be illustrated that increase in additive percentage has reduced HC emission to a greater extent. Neat

biodiesel results in maximum HC emission probably due to less oxygen content compared to blended biodiesel. Furthermore Fig. 6.13a also enumerates that pure triacetin has resulted more reduction in HC emission compared to the experimentally synthesized product containing mixtures of monoacetin, diacetin and triacetin. This can be attributed to the excess O₂ content of triacetin around 53% as reported earlier. This explanation is in compliance with the study made by *Huang et al., 2009*.

6.1.7.2.4 Nitrogen oxide (NO_x) Emission

Formation of NO_x during combustion period is mainly driven by fuel type (high cetane number / high oxygen content) and engine operating conditions. The nitrogen oxide (NO_x) emission for the six different blends of biodiesel and neat biodiesel at different engine speed is given in Fig. 6.13b. Emission of NO_x gradually reduces with increase in engine speed for all the blends as observed from the figure. This can be attributed to the fact that since, peak in-cylinder pressure and temperature are function of a point at which ignition results within the engine cycle; therefore, engine speed directly functionalizes NO_x emission resulting lower NO_x emission at higher speed having lower combustion temperature (*Chong et al., 2015*).

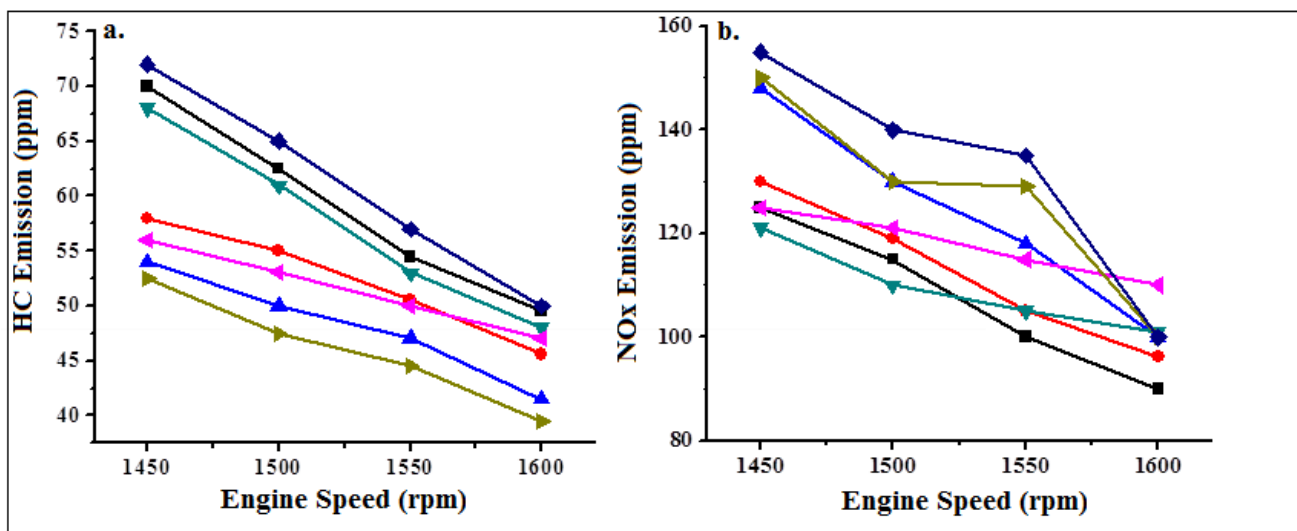


Fig. 6.13. Exhaust emission characteristics for palm biodiesel based diesel engine at different speed for a.

HC and b. NO_x.

6.1.7.3 Engine Performance Analysis

Lower exhaust gas temperature is an indication of complete fuel combustion; Fig 6.14a exhibits that blended fuels resulted lower exhaust gas temperature, depicting complete combustion which has been advocated by lower CO and HC emission (Behçet et al.,2015). Furthermore, brake specific fuel consumption (BSFC) for the blended fuels are comparatively higher than B100 (Fig. 6.14b), because the blended fuels have relatively higher density and lower heating value (Casas et al.,2010). Fig. 6.14c depicts energy in terms of heat input, required in case of B100 to maintain the combustion uniformity whereas additions of CT and ESP display lower heat input which may be accredited to its higher density that results in higher fuel injection rendering more energy release during combustion (Casas et al.,2010). Besides, CT has shown lower heat input compared to ESP because of the presence of monoglycerides and diglycerides in ESP. Brake thermal efficiency (BTE) as visualized from Fig. 6.14d enumerates that addition of CT as well as ESP could result slight improvement in BTE which may due to higher density of the blended fuel (Behçet et al.,2015) compared to B 100.

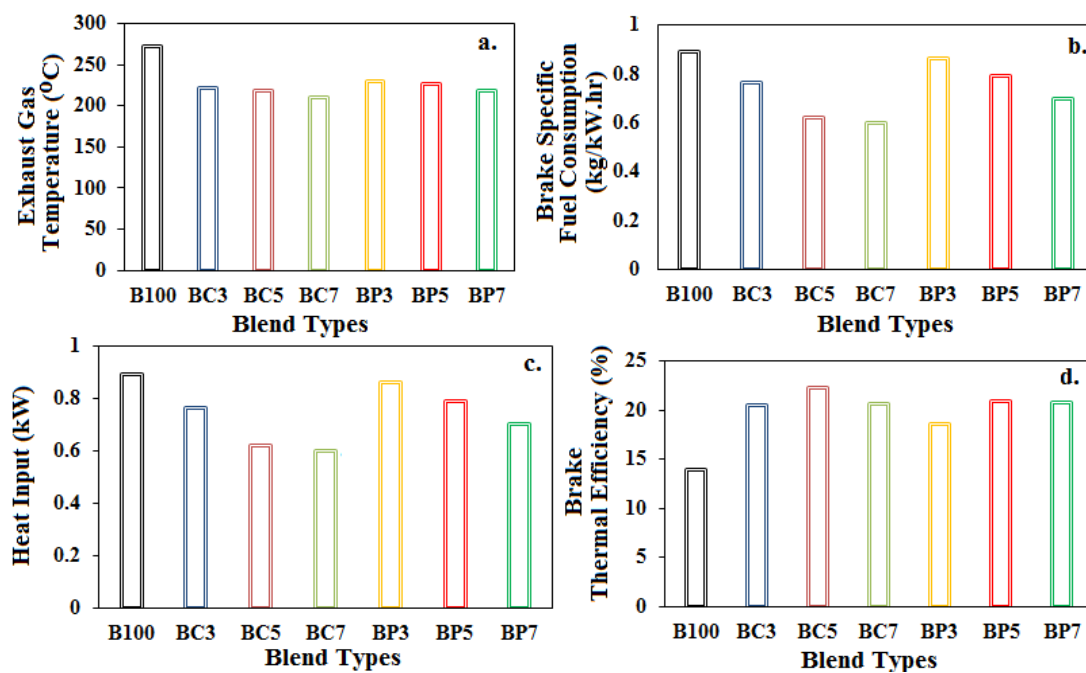


Fig. 6.14. Engine Performance Analysis for different test fuels.

6.1.8 Variation of Engine Performance with engine Speed

6.1.8.1 Brake specific fuel consumption (BSFC)

The brake specific fuel consumption (BSFC) of six different biodiesel-additive blends and neat biodiesel tested in a diesel engine is shown in [Fig. 6.15a](#). The trend shows that with increase in engine speed BSFC for all biodiesel blends increases. However pure biodiesel has also shown similar profile but it has resulted in highest BSFC through out the engine run among all biodiesel blends. This could be well explained by the fact that pure biodiesel has higher density and requires a greater mass than the other biodiesel-additive blends in order to produce the same engine output. This result is in accordance with the study made by *Oner & Altun (2009)*.

6.1.8.2 Brake Thermal Efficiency (BTE)

The variation of brake thermal efficiency (BTE) with engine speed for different biodiesel blends and pure biodiesel is shown in [Fig. 6.15b](#). Brake thermal efficiency indicates how efficiently an engine is extracting energy from fuel and converting it into mechanical energy. The trend shows that with increase in engine speed brake thermal efficiency (BTE) decreases for all biodiesel blends and pure biodiesels. However pure biodiesel has shown lowest efficiency among all the blends. The reason is availability of less oxygen for late combustion period whereas addition of additive in other biodiesel blends has increased oxygen availability resulted in better brake thermal efficiency. Whereas increasing engine speed has resulted in lower residence time for biodiesel blends to convert fuel chemical energy to heat energy thus resulted in lower BTE at higher engine speed (*Chong et al., 2015*).

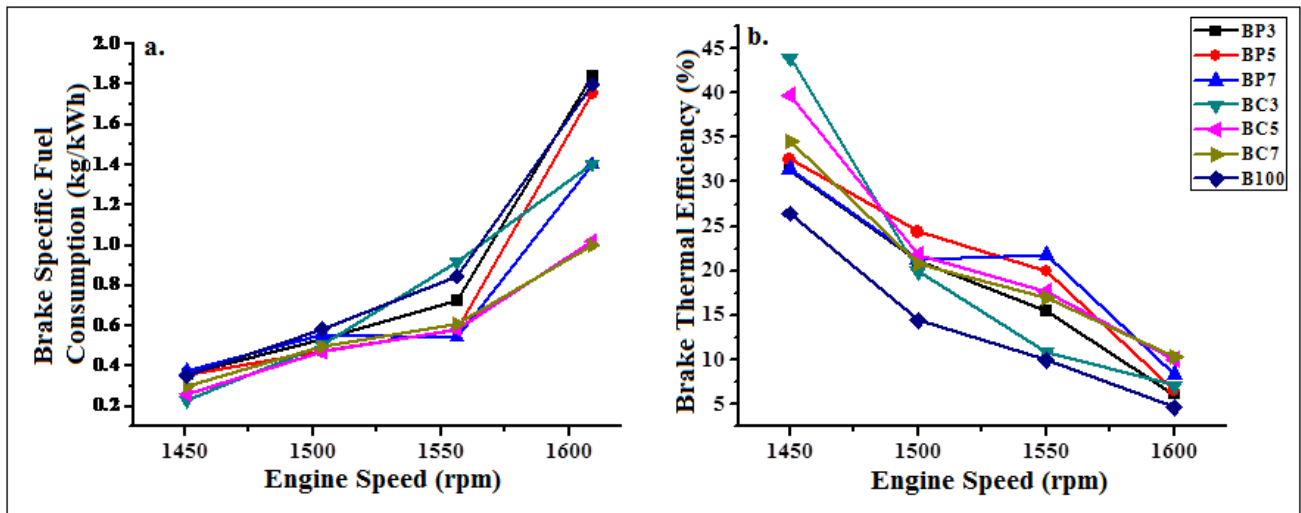


Fig. 6.15. Engine performance for palm biodiesel blends and neat biodiesel at different speed for a. Brake Specific Fuel Consumption b. Brake Thermal Efficiency

6.1.8.3 Heat Input (HI)

Variation in heat input requirement of different biodiesel blend and pure biodiesel with engine speed is given in Fig. 6.16a. The trend shows that with increase in engine speed heat input decreases gradually for all biodiesel blends. Whereas pure biodiesel has shown higher heat requirement than any other biodiesel blends. The possible reason could be availability of more oxygen in blended biodiesel which results in better heat input than pure biodiesel.

6.1.8.4 Exhaust Gas Temperature (EGT)

Fig. 6.16b shows the variation of exhaust gas temperature for all the six biodiesel blends and pure biodiesel tested in a diesel engine with engine speed. In general a lower exhaust gas temperature indicates better combustion and performance (Chauhan et al., 2010). The observation shows that with increase in engine speed exhaust gas temperature decreases for all blends. Except pure biodiesel all biodiesel blends have resulted in a similar EGT profile (260-290 °C) whereas biodiesel has resulted in

maximum EGT of 360 °C. Higher EGT profile shown by pure biodiesel is due to the increased heat loss, which is also clear from its lower brake thermal efficiency compared to all other biodiesel blends (G. Sakthivel et al., 2014). Also the addition of additive into biodiesel blends results in higher availability of oxygen while it decreases the overall energy content of fuel and combined effect of these two results in lower combustion and exhaust temperatures (Yilmaz et al., 2014).

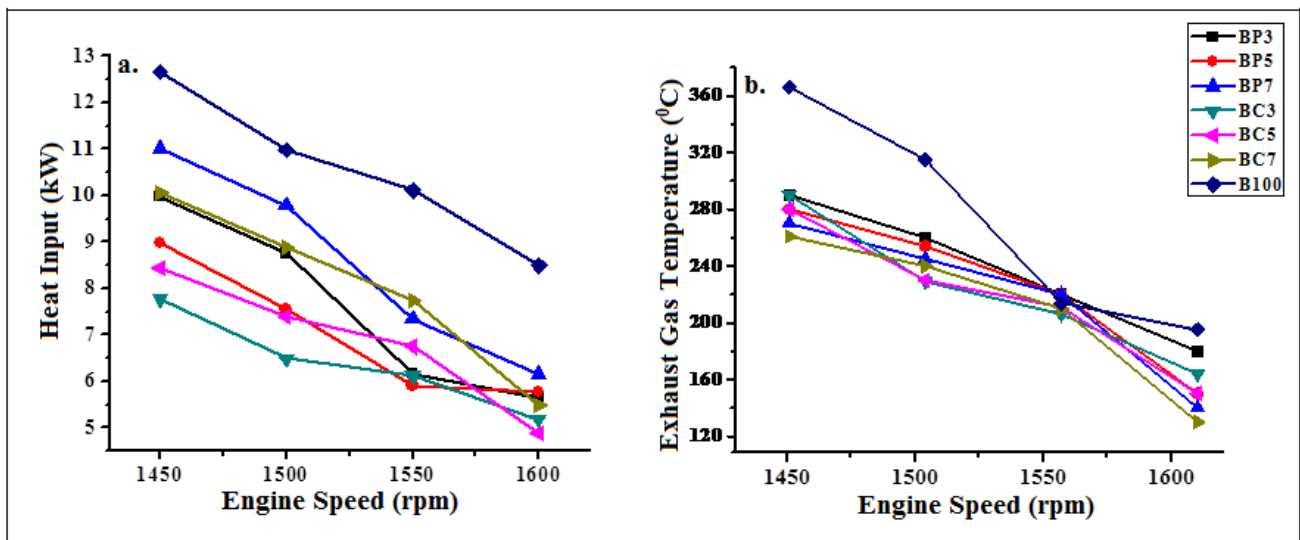


Fig. 6.16. Engine performance for palm biodiesel blends and neat biodiesel at different speed for c. Heat Input and d. Exhaust Gas Temperature.

6.2 Performance and emission analysis of diesel engine fuelled with biodiesel & biodiesel-additive blends (2-Ethyl hexyl acetate and Triacetin)

6.2.1 Comparative study on fuel properties of biodiesel and blended biodiesel

The present work shows the effect of fuel additive on biodiesel property. Triacetin and ethyl hexyl acetate are used as potential fuel additive and they are blended with biodiesel in three different volumetric proportion viz. 1:1, 6:4 and 7:3 respectively. Later these blends were tested in laboratory to study the effect of additive on biodiesel property viz. flash point, pour point, cetane number, density, acid number and viscosity.

6.2.1.1 Effect on Flash point

To study the effect of triacetin (TA) and ethyl hexyl acetate (EHA) on flash point of biodiesel three different blends were prepared with varying proportion of triacetin and ethyl hexyl acetate. The obtained response is shown in [Fig. 6.17a](#). The trend shows that with increase in EHA percentage in biodiesel blend flash point of the mixture decreases whereas the effect of TA is negligible. This could be explained by the fact that EHA itself has low flash point at 75⁰C which reduces flash point of pure biodiesel (164⁰C) significantly (*Vedaraman et al., 2011*). Thus further addition of EHA above a certain ratio in biodiesel additive has been restricted.

6.2.1.2 Effect on Pour point

The effect of triacetin (TA) and ethyl hexyl acetate (EHA) on biodiesel blends are shown in [Fig. 6.17b](#). Three different biodiesel blends were formulated using TA & EHA in different proportion. Pure palm biodiesel has a pour point of 18⁰C (laboratory tested). The trend shows that addition of additive has resulted in a decrease in pour point of pure biodiesel. The fact is that branched alcohols are well known for their pour point reduction. EHA has its freezing point at -93⁰C whereas TA has -71⁰C (*Hancock et al., 1948*). So a mixture of these two has resulted in appreciable reduction of 4⁰C when blended in 7:3

ratio with biodiesel (*Casas et al., 2010*). Thus this particular blend of triacetin and ethyl hexyl acetate could be used as a potential cold flow improver and enabling biodiesel to be used in cold climate.

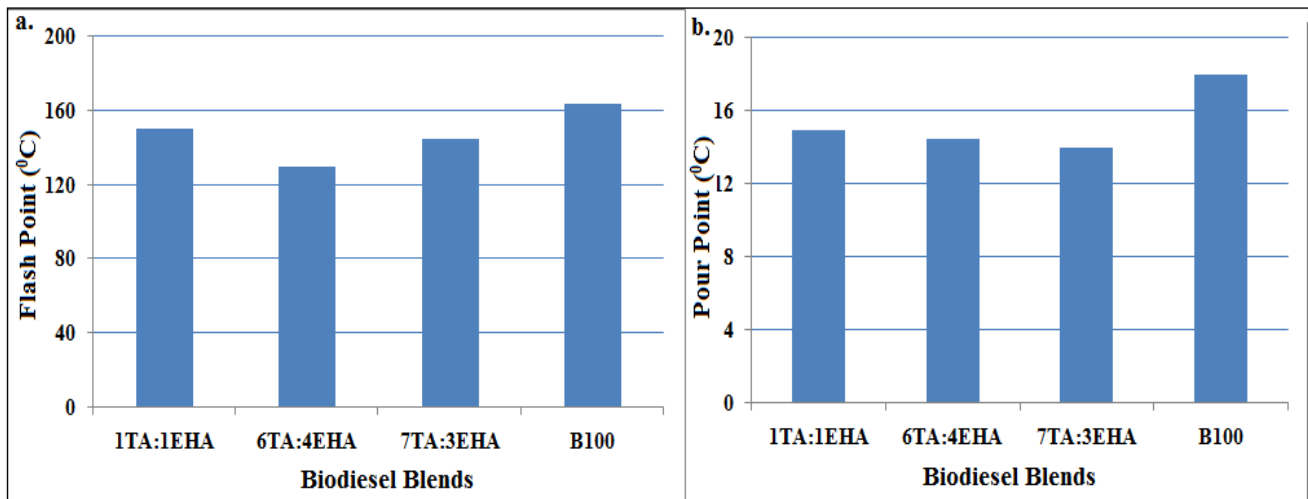


Fig. 6.17. Effect of additive on different biodiesel blends a. Flash Point b. Pour Point

6.2.1.3 Effect on Cetane number

Effect on cetane number of palm biodiesel after the addition of triacetin and ethyl hexyl acetate is shown in Fig. 6.18a. Cetane number is a measure to examine diesel engine performance and it is defined as the mixture of cetane and isocetane that possesses the same ignition delay. Higher the cetane number lesser will be the ignition delay and better will be the engine performance. Our study shows that addition of additive has resulted in a reduction in cetane number. When TA and EHA blended in a proportion of 1:1 it has resulted in a very close value of 64.1 to 65 of pure biodiesel. This result could be explained by the fact that TA and EHA have cetane number of 15 and 48 respectively which on addition has resulted in a reduction (*Knothe et al., 2003*).

6.2.1.4 Effect on Density

Effect of triacetin and ethyl hexyl acetate on density of palm biodiesel is represented in Fig. 6.18b. Density of a fuel is an important parameter to regulate the quantity of fuel to be injected and

performance of an engine during combustion (*Knothe et al., 2005*). The study shows that addition of TA and EHA has resulted in an increase in density of biodiesel in the range of 880-891 kg/m³ whereas density of palm biodiesel is at 875 kg/m³. The fact that EHA has a density of 870 kg/m³ similar to biodiesel has very negligible effect on blended biodiesel whereas the effect of TA on blended biodiesel is more prominent because of the fact that TA has a density of 1160 kg/m³ and thus an increase in triacetin proportion increases density of biodiesel blend (*Garcia et al., 2008*).

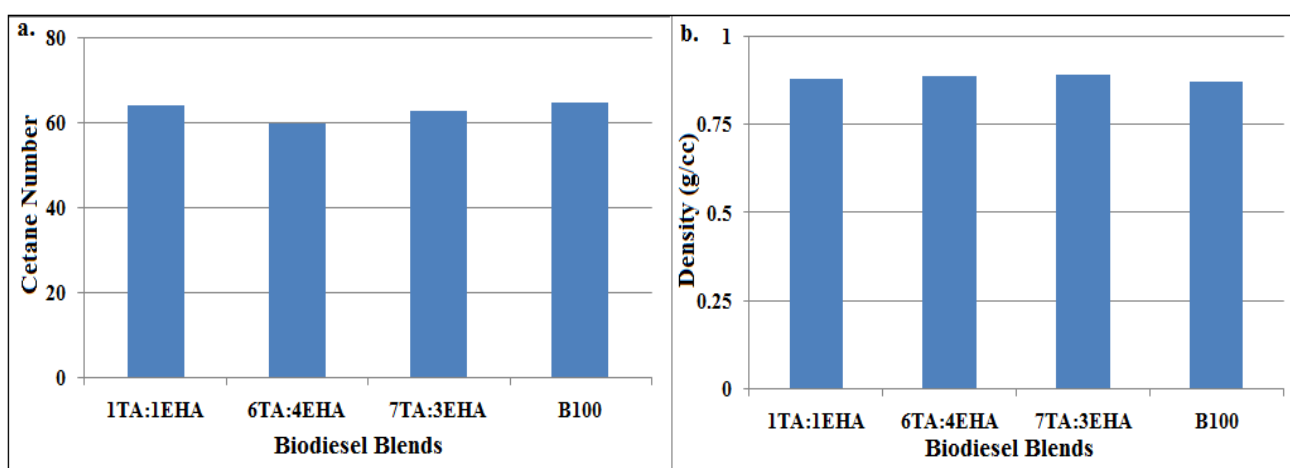


Fig. 6.18. Effect of additive on biodiesel property a. Cetane number b. Density

6.2.1.5 Effect on Viscosity

Triacetin (TA) and ethyl hexyl acetate (EHA) are mixed with palm biodiesel in three different proportions and their effect is shown in Fig. 6.19a. Kinematic viscosity is an important parameter which regulates the quantity of a fuel to be injected and combustion of a fuel. An increased viscosity causes choking in fuel line and leads to poor combustion due to insufficient supply of fuel in engine and finally results in increased temperature and NO_x emission (*Mittelbach et al., 2004*). The present trend shows that additives have a very marginal effect on biodiesel viscosity which lies in the range of 4.5-4.91 cSt whereas Palm biodiesel has a viscosity of 4.482 cSt at 40⁰C. This result can be attributed to the fact that

triacetin has viscosity at 7.83 cSt which is much higher than biodiesel, is compensated by EHA which has density at 1.15 cSt and thus it has resulted in a similar viscosity to biodiesel (*Saka & Isayama, 2009*).

6.2.1.6 Effect on Acid value

Effect of triacetin and ethyl hexyl acetate on acid value of biodiesel is shown on Fig. 6.19b. Acid value of a fuel is calculated to characterize its stability during storage. The present study shows on increasing additive proportion there is a slight increase in acid value however it remains under tolerance limit of 0.56 mg KOH/g set by European standard (EN 14104)(*Garcia et al., 2008*). Thus it is evident from the study that application of TA and EHA doesn't affect acid value of biodiesel and can be used as a potential oxygenated additive.

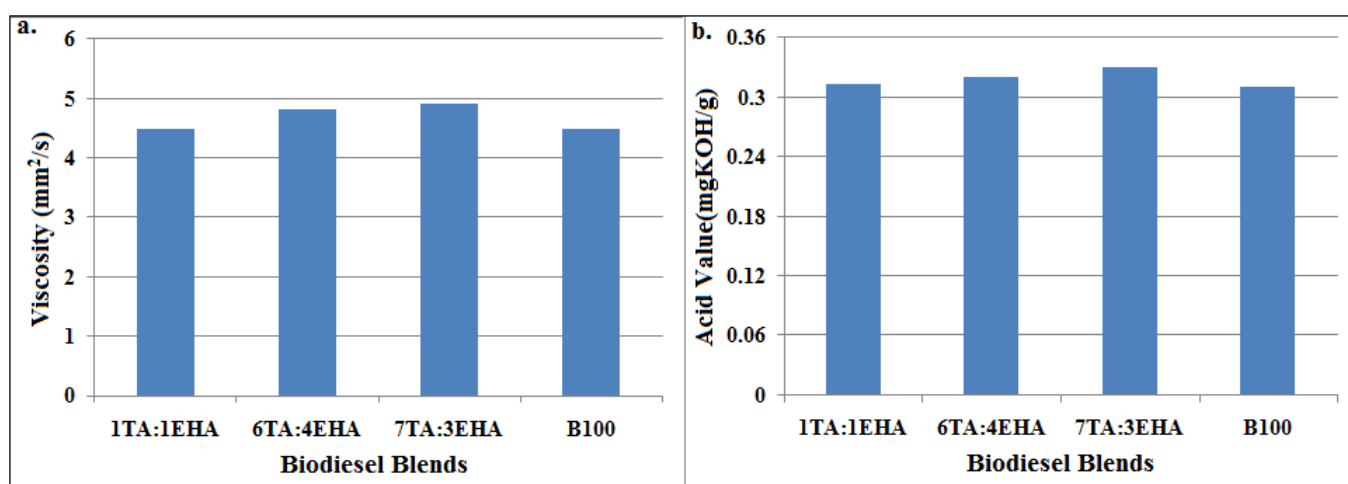


Fig. 6.19. Effect of additive on biodiesel property a. Viscosity b. Acid value

6.2.2 Comparative study on diesel engine emission fuelled with biodiesel and blended biodiesel

Three different biodiesel blends were formulated using triacetin (TA) and ethyl hexyl acetate (EHA) in the ratio of 1:1, 6:4 and 7:3 (vol.%). Then their performance in terms of emission was tested in a diesel engine.

6.2.2.1 Carbon monoxide (CO) emission

Incomplete combustion of fuel results in generation of carbon monoxide. As depicted from the [Fig. 6.20a](#) the general trend shows that with increase in engine speed CO emission decreases. B100 shows maximum CO emission whereas, in case of blended fuels, increase in vol. percent of TA (from 1 vol % to 7 vol. %) in the mixed blend resulted decrease in CO emission due to its higher oxygen content. This signifies complete combustion. Furthermore, increase in engine speed prevents the formation of rich fuel zone which thus enables complete transformation of CO to CO₂ (*Liaquata et al., 2012*).

6.2.2.2 Carbon dioxide (CO₂) emission

Lower CO emission is representative of higher CO₂ emission which signifies complete combustion. Therefore B100 showing comparatively more CO emission in [Fig. 6.20a](#) depicts lower CO₂ emission in [Fig. 6.20b](#) compare to the blended fuels. Similarly increase in TA vol% enumerated complete combustion and demonstrated more or less linear function of engine speed. This can be attributed to the fact that increase in TA % has increased the oxygen content of the blended fuel causing earlier combustion rendering more time for transformation of CO to CO₂ thus resulting 13% and 20.6% increase in CO₂ emission compared to B100 (*Puhan et al., 2005*).

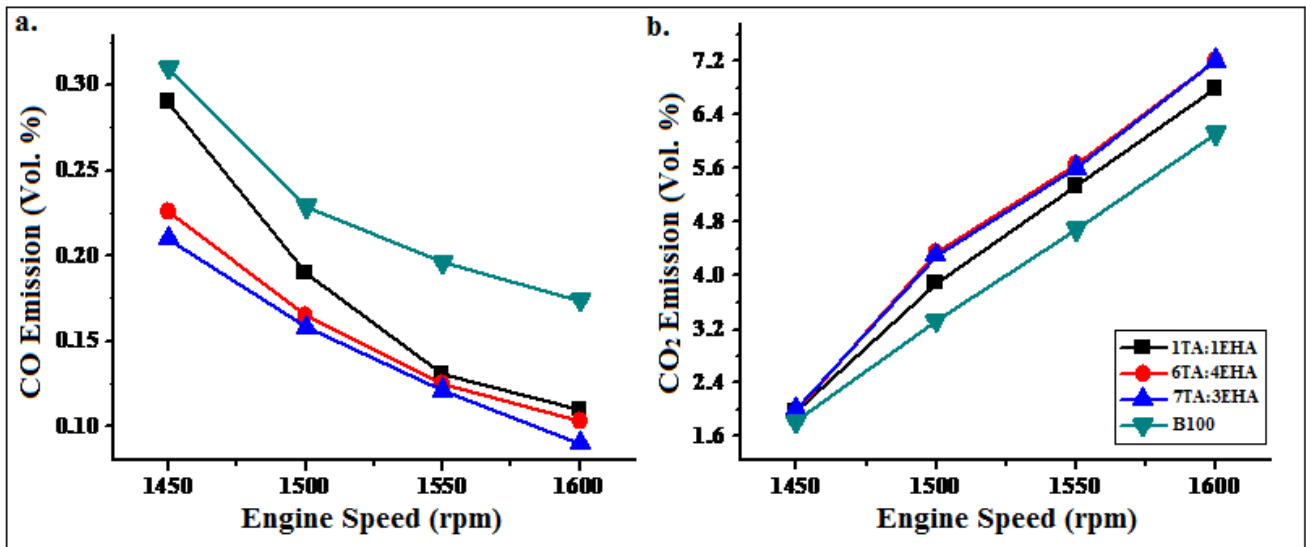


Fig. 6.20. Exhaust emission variation with engine speed fuelled with blended biodiesel in diesel engine for
a. CO emission b. CO₂ emission

6.2.2.3 Nitrogen oxide (NO_x) emission

Formation of nitrogen oxide (NO_x) occurs during combustion stage and it is mainly governed by fuel type and engine operating conditions. Emissions of NO_x clearly reduce with increasing engine speed, regardless of fuel type. This is due to the fact that peak in-cylinder pressure and temperature are dependent on at which point ignition occurs within the engine cycle, rather than the absolute time, it explains why for the lower engine speed has higher NO emissions (*Chong et al., 2015*). Since, B100 has higher cetane number results in rapid combustion that leads to higher peak pressure and in-cylinder temperature resulting higher NO_x emission compared to blended fuels. Furthermore, it can well be identified from the Fig.6.21a that increase in EHA vol. % in the mixed blend results lower NO_x emission which may be due to slower burning of the fuel having low cetane number.

6.2.2.4 Hydrocarbon (HC) emission

Emission of the unburned hydrocarbon (UHC) under different operating speeds has been represented in Fig. 6.21b. UHC is found to decrease with increasing engine speed. The reason for lower HC emissions

can be due to the higher oxygen content in fuel blends, which helps to complete oxidations in rich air-fuel mixture zones by increasing the oxidation reaction ratio. Interestingly increase in EHA content in the blends from 1vol.% ,3vol%,and 4vol% resulted in reduction of UHC by 8.55%, 12.27%, and 14.535 % respectively whereas, B100 although have higher cetane number show higher UHC since initial incorporation of oxygen molecules present in B100 results in localized burning thus resulting generation of UHC (*Song et al., 2006*).

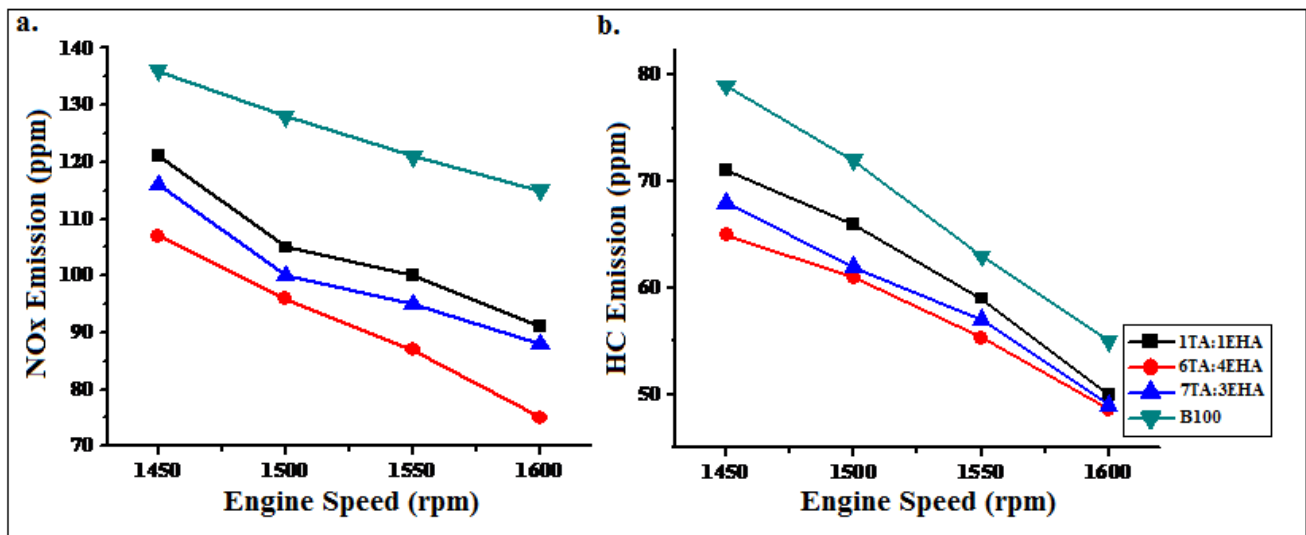


Fig. 6.21. Exhaust emission variation with engine speed fuelled with blended biodiesel in diesel engine for
a. NOx emission b. HC emission

6.2.3 Comparative study on engine performance fuelled with biodiesel and blended biodiesel

6.2.3.1 Exhaust Gas Temperature (EGT)

In analyzing the emission characteristics of a diesel engine the exhaust gas temperature is an important indicator of the heat of the fuels tested at the combustion period. The variation of exhaust gas temperature with respect to engine speed for the tested fuels is shown in Fig. 6.22a. The emission measurements were taken for approximately three minutes after the temperature and emissions quantities stabilize for a given engine operating condition (*Chong et al., 2015*). It can be observed in this

figure that increase in triacetin (TA) blend proportion has resulted reduction in exhaust gas temperature of fuel since the fuel constitutes around 53% oxygen content which has also been evidenced by lower CO emission. Furthermore the blended fuel resulted in max 25% reduction in EGT compared to B100 depicting complete combustion.

6.2.3.2 Brake Thermal Efficiency (BTE)

[Fig. 6.22b](#) shows effect of engine speed on brake thermal efficiency of a diesel engine fuelled with three different blends of biodiesel and pure biodiesel. One of the main problems in diesel engine combustion despite its lean operating nature is the low availability of localized oxygen at the late combustion phase. This is due to the mixing-controlled combustion phase at the end having consumed most of the oxygen in the vicinity. The oxygenated fuel blends supplies oxygen at the late combustion phase thus resulting improved brake thermal efficiency. Since TA contains major amount of oxygen hence, it shows better brake thermal efficiency compared to B100. It can also be revealed from the [Fig. 6.22b](#) that only increase in TA vol % has resulted high brake thermal efficiency. However, increase in engine speed results in decrease in brake thermal efficiency due to less residence time for conversion of chemical energy of fuel into heat energy (*Silitonga et al., 2013*).

6.2.3.3 Brake Specific Fuel Consumption (BSFC)

The brake specific fuel consumption (BSFC) of three different blends of biodiesel and neat biodiesel under different operating speeds is shown in [Fig. 6.22c](#). The general trend shows that with increase in engine speed BSFC increases for all blend types. From the figure it can be concluded that no such improvement in BSFC of B100 and blended biodiesel at lower engine speed whereas slight increase in BSFC is observed in blended fuels due to lower cetane number and higher densities. Biodiesel blend containing TA to EHA 7:3 (vol. %) has resulted in higher BSFC throughout engine run however,

increase in EHA content has resulted decrease in density and viscosity of the blend biodiesel resulting better fuel atomization rendering slight improvement in BSFC (*Vallinayagam et al., 2014*).

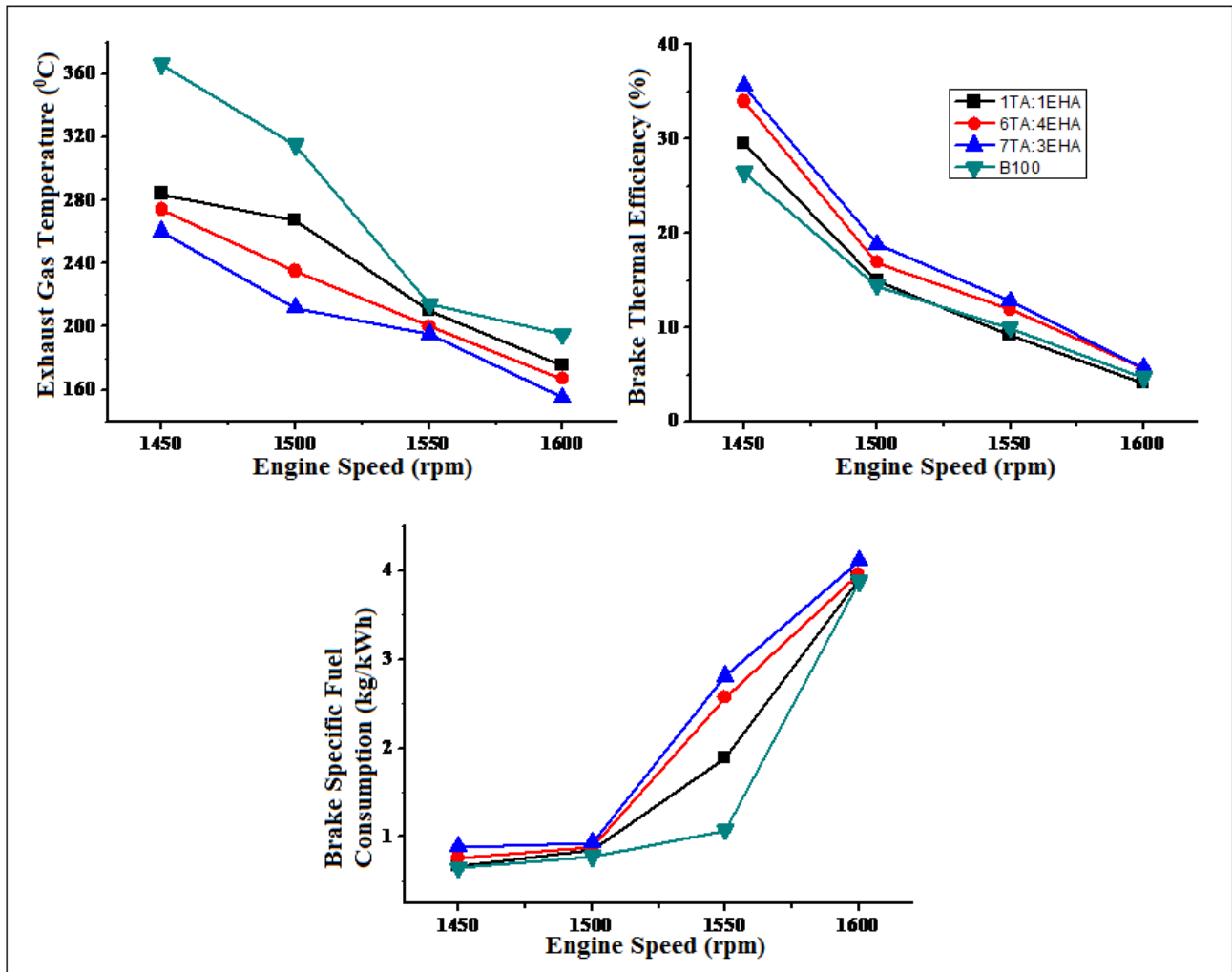


Fig. 6.22. Engine performance of diesel engine fuelled by palm biodiesel blends and neat biodiesel at different speed for a. Brake Specific Fuel Consumption b. Brake Thermal Efficiency and c. Exhaust Gas Temperature.

CHAPTER-7

CONCLUSION

7. Conclusion

7.1 Glycerol acetic acid esterification with pork bone supported antimony HAp catalyst

The present study demonstrates successful application of pork bone as a source of catalyst support for subsequent application in synthesis of commercially important fuel additives. The prepared catalyst exhibited good stability and resulted good reusability for subsequent eight experimental trials with uninterrupted glycerol conversion and diacetin, triacetin selectivity. Noticeably, an energy-efficient infrared excitation could result much higher combined selectivity of diacetin and triacetin compared to conventional heating within a significantly shorter reaction time of 2h thus implicating energy efficacy of infrared radiation over conventional heating. Taguchi optimization could adequately identify the most significant parameters affecting desired product yield. Remarkably, the optimally synthesized product developed through energy-efficient infrared radiation, exhibited equivalent potency in comparison with commercially available product in terms of fuel properties, engine performance and emission attributes.

7.2 Emission and performance study of diesel engine fuelled with TA-EHA-Biodiesel blend

Blend of triacetin and 2-ethyl hexyl acetate has remarkable effect on pour point. It has resulted in appreciable reduction in pour point and NO_x emission, however very slight reduction has been observed in other emissions and other engine performance parameters (brake specific fuel consumption and brake thermal efficiency). Additionally, excess addition results in lowering of cetane number. This can be attributed to the fact that a single additive cannot improve all the fuel properties therefore, an additional blend is required which will be able to amplify the fuel performance.

CHAPTER-8

FUTURE SCOPE OF WORK

8. FUTURE SCOPE OF WORK

1. Apart from antimony (Sb) different transition metals viz. Ti, Vd can be impregnated on HAp support to derive cost effective catalyst which could have better performance.
2. Developed Sb_HAp catalyst can possibly be applied in other glycerol based esterification reactions.
3. Determination of reaction kinetics is one important task to be completed.
4. Existing reaction has been carried out in a batch reactor and it can be conducted in catalytic packed bed reactor.
5. To make the esterification process even more cost effective different intensification methods could be applied and compared.
6. In this present work cost effective catalyst has been developed from synthesis of municipal solid waste so this idea could be actualized to produce cost effective catalyst on industrial scale.

CHAPTER-9

REFERENCES

9. REFERENCES

- [1] Adaileh MW, AlQdah KS. Performance of diesel engine fuelled by a biodiesel extracted from a waste cooking oil, *Energy Procedia* 18 (2012) 1317–1334.
- [2] Aleklett K, Höök M, Jakobsson K, Lardelli M, Snowden S, Söderbergh B. The peak of the oil age analyzing the world oil production reference scenario in world energy outlook 2008. *Energy Policy* 2010; 38:1398–414.
- [3] Andrade-Tacca CA, Chang CC, Chen Y, Manh D, Chang CY, Ji DR, Tseng JY, Shie JL. Esterification of jatropha oil via ultrasonic irradiation with auto-induced temperature-rise effect. *Energy*. 2014;71: 346–354.
- [4] Ashraful AM, Masjuki HH, Kalam MA, Rizwanul Fattah IM, Imtenan S, Shahir SA. Production and comparison of fuel properties, engine performance, and emission characteristics of biodiesel from various non-edible vegetable oils: a review. *Energy Convers Manage*. 2014;80:202–28.
- [5] Bagby MO. Vegetable oils for diesel fuel: opportunities for development. *Am Soc Agric Eng* .1987;87-1588.
- [6] Balaraju M, Nikhitha P, Jagadeeswaraiiah K, Srilatha K, Prasad PSS, Lingaiah N. Acetylation of glycerol to synthesize bioadditives over niobic acid supported tungstophosphoric acid catalysts. *Fuel Process Technol* 2010; 91: 249–53.
- [7] Banapurmath NR, Tewari PG, Hosmath RS. Performance and emission characteristics of a DI compression ignition engine operated on Honge, Jatropha and sesame oil methyl esters. *Renew Energy* 2008; 33:1982–8.

- [8] Batt RJ, McMillan JA, Bradbury I. Lubricity additives-performance and noharm effects in low sulfur fuels. SAE Technical Paper; 1996.
- [9] Behçet R, Oktay H, Çakmak A, Aydın H. Comparison of exhaust emissions of biodiesel–diesel fuel blends produced from animal fats. *Renew Sust Energ Rev* 2015; 46: 157–65.
- [10] Bouyer E, Gitzhofer F, Boulos MI. Morphological study of hydroxyapatite nanocrystal suspension. *J Mater Sci: Mater Med.* 2000; 11: 523-531.
- [11] Bowman M, Hilligoss D, Rasmussen S, Thomas R. Biodiesel: a renewable and biodegradable fuel. *Hydrocarbon Process.* 2006;85:103-6.
- [12] Buasri A, Inkaew T, Kodephun L, Yenying W, Loryuenyon V. Natural Hydroxyapatite (NHAp) Derived from Pork Bone as a Renewable Catalyst for Biodiesel Production via Microwave Irradiation. *Key Engineering Materials.*2015; 659 :216-220.
- [13] Buasri A, Rattanapan T, Boonrin C, Wechayan C, Loryuenyong V. Oyster and Pyramidella Shells as Heterogeneous Catalysts for the Microwave-Assisted Biodiesel Production from *Jatropha curcas* Oil. *J Chem.*2015. Article ID 578625.
- [14] Cai R, Wang H, Cao M, Hao L, Zhai L, Jiang S, Li X. Synthesis and antimicrobial activity of mesoporous hydroxylapatite/zinc oxide nanofibers. *Mater Design.*2015;87: 17-24.
- [15] Canakci M, Gerpen JHV, Comparison of engine performance and emission for petroleum diesel fuel, yellow grease biodiesel, and soyabean oil biodiesel. *American Society of Agricultural Engineers* 2003; 46(4): 937–944.
- [16] Casas A, Ruiz JR, Ramos MJ, Perez A. Effects of Triacetin on Biodiesel Quality. *Energy Fuels* 2010; 24: 4481–89

- [17] Chakraborty R, Mandal E. Fast and energy efficient glycerol esterification with lauric acid by near and far-infrared irradiation: Taguchi optimization and kinetics evaluation. *J Taiwan Inst Chem Eng* 2015; 50: 93–9.
- [18] Chakraborty R, Bepari S, Banerjee A. Application of calcined waste fish (*Labeo rohita*) scale as low-cost heterogeneous catalyst for biodiesel synthesis. *Bioresour. Technol.* 2011;102:3610–3618.
- [19] Chakraborty R, Bepari S, Banerjee A. Transesterification of soybean oil catalyzed by fly ash and egg shell derived solid catalysts. *Chem. Eng. J.* 2010;165:798–805.
- [20] Chakraborty R, D SK. Optimization of Biodiesel Synthesis from Waste Frying Soybean Oil Using Fish Scale-Supported Ni Catalyst. *Ind. Eng. Chem. Res.*, 2012;51 (25):8404–8414.
- [21] Chakraborty R, Das S, Bhattacharjee SK. Optimization of biodiesel production from Indian mustard oil by biological tri-calcium phosphate catalyst derived from turkey bone ash. *Clean Techn Environ Policy* 2015; 17: 455-63.
- [22] Chakraborty R, RoyChowdhury D. Fish bone derived natural hydroxyapatite-supported copper acid catalyst: Taguchi optimization of semibatch oleic acid esterification. *Chem. Eng. J.* 2013;215–216:491–499.
- [23] Chakraborty R, RoyChowdhury D. Optimization of biological-hydroxyapatite supported iron catalyzed methyl oleate synthesis using response surface methodology. *J Taiwan Inst Chem Eng* 2014; 45: 92-100.
- [24] Chakraborty R, Sahu H. Intensification of biodiesel production from waste goat tallow using infrared radiation: Process evaluation through response surface methodology and artificial neural network. *Appl Energ.* 2014;114: 827–836.

- [25] Chauhan BS, Kumar N, Du Jun Y, Lee KB. Performance and emission study of preheated Jatropha oil on medium capacity diesel engine. *Energy* 2010; 35:2484– 92.
- [26] Chong CT, Ng J-H, Ahmad S, Rajoo S. Oxygenated palm biodiesel: Ignition, combustion and emissions quantification in a light-duty diesel engine. *Energ convers manage*. 2015;101:317–325.
- [27] Chowdhury A, Chakraborty R, Mitra D, Biswas D. Optimization of the production parameters of octyl ester biolubricant using Taguchi's design method and physico-chemical characterization of the product. *Ind Crops and Prod*. 2014; 52:783–89.
- [28] Christoph R, Schmidt B, Steinberner U, Dilla W, Karinen R, Ullmann's Encyclopedia of Industrial Chemistry Published by Wiley-VCH, Weinheim. 2006.
- [29] Clacens JM, Pouilloux Y, Barrault J. Selective etherification of glycerol to polyglycerols over impregnated basic MCM-41 type mesoporous catalysts. *Appl Catal A*. 2002;227:181–90.
- [30] Darabi HR, Aghapoor K, Taala F. Silica-Supported Antimony(III) Chloride as Highly Effective and Reusable Heterogeneous Catalyst for the Synthesis of Quinoxalines. *Cat Lett*. 2009; 133: 84-9.
- [31] Da-Silva GP, Mack M, Contiero J. Glycerol: a promising and abundant carbon source for industrial microbiology. *Biotechnol Adv*. 2009;27:30-9.
- [32] Dosuna-Rodriguez I, Adriany C, Gaigneaux EM. Glycerol acetylation catalysed by ion exchange resins. *Catal. Today* 2011; 167: 56–63.
- [33] Duh B. Effect of antimony catalyst on solid-state polycondensation of poly(ethylene terephthalate). 2002;43:3147-3154.

- [34] Dunn RO, Knothe G. Alternative diesel fuels from vegetable oils and animal fats. *J Oleo Sci* 2001; 50(5):415–26
- [35] Fattah IMR, Masjuki HH, Kalam MA, Wakil MA, Ashraful AM, Shahir SA. Experimental investigation of performance and regulated emissions of a diesel engine with *Calophyllum inophyllum* biodiesel blends accompanied by oxidation inhibitors. *Energy Convers Manage.* 2014;83:232–40.
- [36] Fernando S, Hall C, Jha S. NO_x reduction from biodiesel fuels. *Energy Fuel.* 2006; 20:376-82.
- [37] Ferreira P, Fonseca IM, Ramos AM, Vital J, Castanheiro JE. Esterification of glycerol with acetic acid over dodecamolybdophosphoric acid encaged in USY zeolite. *Catal Commun.* 2009;10:481-4.
- [38] Forester DR, Robert SDC, Manka JS, Malik BB. Jet fuel additive concentrate composition and fuel composition and methods thereof. US Patent WO.2003106595; 2003.
- [39] Galhardo TS, Simone N, Goncalves M, Figueiredo FCA, Mandelli D, Carvalho WA. Preparation of Sulfonated Carbons from Rice Husk and Their Application in Catalytic Conversion of Glycerol. *ACS Sustainable Chem. Eng* 2013; 1:1381–89.
- [39] Gao D, Yin H, Wang A, Shen L, Liu S. Gas phase dehydrogenation of ethanol using maleic anhydride as hydrogen acceptor over Cu/hydroxylapatite, Cu/SBA-15, and Cu/MCM-41 catalysts. *J Ind Eng Chem.* 2015;26: 322–332.
- [40] García E, Laca M, Perez E, Garrido A, Peinado J. New Class of Acetal Derived from Glycerin as a Biodiesel Fuel Component. *Energy Fuels* 2008; 22: 4274–80.
- [41] Gerhard Knothea, Andrew C. Matheausb, Thomas W. Ryan III *Fuel* 82 (2003) 971–975
- Giraldo SY, Rios LA, Franco A, Cardeño F. Synthesis of additives for biodiesel through chemical modifications of glycerol. *Inf Technol* 2009; 20:75–84.

- [42] Giraldo SY, Rios LA, Suárez N. Comparison of glycerol ketals, glycerol acetates and branched alcohol-derived fatty esters as cold-flow improvers for palm biodiesel. *Fuel* 2013;108:709–714.
- [43] Gonçalves VLC, Pinto BP, Silva JC, Mota CJA. Acetylation of glycerol catalyzed by different solid acids. *Catal Today*. 2008;133-135:673-7.
- [44] Hajamini Z, Sobati MA, Shahhosseini S. Waste fish oil (WFO) esterification catalyzed by sulfonated activated carbon under ultrasound irradiation. *Appl Therm Eng*. 2016; 94:1-10.
- [45] Hasan Z, Yoon JW, Jung SH. Esterification and acetylation reactions over in situ synthesized mesoporous sulfonated silica *Chem. Eng. J*. 2015; 278: 105–12.
- [46] Hemerski F, Corazza M. LDH-catalyzed esterification of lauric acid with glycerol in solvent free system. *Appl Catal A: Gen* 2014;475:242-8.
- [47] Hermida L, Abdullaha AZ, Mohameda AR. Synthesis of monoglyceride through glycerol esterification with lauric acid over propyl sulfonic acid post-synthesis functionalized SBA-15 mesoporous catalyst. *Chem Eng J* 2011;174:668-76.
- [48] Hoekman SK, Broch A, Robbins C, Cenicerros E, Natarajan M. Review of biodiesel composition, properties, and specifications. *Renew Sustain Energy Rev*. 2012;16:143–69.
- [49] Hoo P, Abdullah A. Direct synthesis of mesoporous 12-tungstophosphoric acid SBA-15 catalyst for selective esterification of glycerol and lauric acid to monolaurate. *Chem Eng J* 2014;250:274-87.
- [50] Hu W, Zhang Y, Huang Y, Wang J, Gao J, Xu J. Selective esterification of glycerol with acetic acid to diacetin using antimony pentoxide as reusable catalyst. *J Energy Chem* 2015; 5: 632-36.

- [51] Huang J, Wang Y, Li S, Rosilly AP, Yu H, Li H. Experimental investigation on the performance and emissions of a diesel engine fuelled with ethanol–diesel blends. *Appl. Therm. Eng.* 2009;29: 2484–2490.
- [52] Huang J, Wang L-C, Liu Y-M, Cao Y, He H-Y, Fana K-N. Gold nanoparticles supported on hydroxylapatite as high performance catalysts for low temperature CO oxidation. *Appl. Catal., B: Environmental.* 2011;101:560–569.
- [53] Jamroz ME, Jarosz M, Witowska-Jarosz J, Bednarek E, Tecza W, Jamroz MH, et al. Mono-, di-, and tri-tert-butyl ethers of glycerol: a molecular spectroscopic study. *Spectrochim Acta: A Mol Biomol Spectrosc* 2007;67:980–8.
- [54] Jayathilakan K, Sultana K, Radhakrishna K, Bawa AS. Utilization of byproducts and waste materials from meat, poultry and fish processing industries: a review. *J Food Sci Technol.* 2012;49: 278–293.
- [55] Joshi G, Lamba BY, Rawat DS, Mallick S, Murthy K. Evaluation of additive effects on oxidation stability of *Jatropha curcas* biodiesel blends with conventional diesel sold at retail outlets. *Ind Eng Chem Res.* 2013;52:7586–92.
- [56] Joshi RM. Flow properties of biodiesel fuel blends at low temperatures. *Fuel.* 2007;86:143–51.
- [57] Kalam MA, Masjuki HH. Testing palm biodiesel and NPAA additives to control NO_x and CO while improving efficiency in diesel engines. *Biomass Bioenerg* 2008; 32: 1116-22.
- [58] Kang K, Azargohar R, Dalai AK, Wang H. Hydrogen production from lignin, cellulose and waste biomass via supercritical water gasification: Catalyst activity and process optimization study. *Energy Convers. Manage* 2016; 117: 528–37.

- [59] Kantharia N, Naik S, Apte S, Kheur M, Kheur S, Kale B. Nano-hydroxyapatite and its contemporary applications. *J Dent Res Sci Develop.* 2014;1(1):15.
- [60] Kapoor M, Gupta M.N. Obtaining monoglycerides by esterification of glycerol with palmitic acid using some high activity preparations of *Candida antarctica* lipase B. *Process Biochemistry* 47 (2012) 503-508.
- [61] Karavalakis G, Hilari D, Givalou L, Karonis D, Stournas S. Storage stability and ageing effect of biodiesel blends treated with different antioxidants. *Energy.* 2011;36:369–74.
- [62] Kenkel P, Holcomb R. Feasibility of on-farm or small scale oilseed processing and biodiesel. In: English BC, Menard J, Jensen K, editors. *Integration of agricultural and energy systems.* Atlanta, Georgia: Global Bioenergy Partnership; 2008.
- [63] Khayoon MS, Hameed BH. Synthesis of hybrid SBA-15 functionalized with molybdophosphoric acid as efficient catalyst for glycerol esterification to fuel additives. *Appl. Catal A* 2012; 433-434:152-61.
- [64] Kiss NZ, Keglevich G. Microwave-assisted direct esterification of cyclic phosphinic acids in the presence of ionic liquids. *Tel L:* 2016; 16:30044-2.
- [65] Klepa'cova' K, Mravec D, Kaszonyi A, Bajus M. Etherification of glycerol and ethylene glycol by isobutylene. *Appl Catal A* 2007;328:1-13.
- [66] Kolmetz K, Ng WK, Faessler PW. Optimize process operation with new vacuum distillation methods. *Hydrocarbon Process.* 2005;84:77-85.

- [67] Konwar LJ, Mäki-Arvela P, Begum P, Kumar N, Thakur AJ, Mikkola JP, Deka RC, Deka D. Shape selectivity and acidity effects in glycerol acetylation with acetic anhydride: Selective synthesis of triacetin over Y-zeolite and sulfonated mesoporous carbons. *J. Catal.* 2015; 329: 237–47
- [68] Lacerda CV, Carvalho MJS, Ratton AR, Soares IP, Borges LEP. Synthesis of Triacetin and Evaluation on Motor. *J. Braz. Chem. Soc.* 2015; 8: 1625-31.
- [69] Lee JS, Park JY, Kim DK, Lee JP, Park SC, Kim YJ. Blending effects of biodiesels on oxidation stability and low temperature flow properties. *Bioresour. Technol.* 2008; 99: 1196 –203.
- [70] Liao X, Zhu Y, Wang SG, Li Y. Producing triacetyl glycerol with glycerol by two steps: Esterification and acetylation. *Fuel Process Technol* 2009; 90: 988–93.
- [71] Lieu T, Yusup S, Moniruzzaman M. Kinetic Study on Microwave-Assisted Esterification of Free Fatty Acids derived from Ceiba Pentandra Seed Oil. *Bioresour Technol.* 2016;16:30408-4.
- [72] Lin CY, Chen WC. Effects of potassium sulfide content in marine diesel fuel oil on emission characteristics of marine furnaces under varying humidity of inlet air. *Ocean Eng.* 2006;33:1260-70.
- [73] Liu X, Ma H, Wu Y, Wang C, Yang M, Yan P, Welz-Biermann U. Esterification of glycerol with acetic acid using double SO₃H-functionalized ionic liquids as recoverable catalyst. *Green Chem.* 2011; 13: 697–701
- [74] Liu Y, Yuan X, Wang H, Chen X, Gu S, Jiang Q, Wu Z, Jiang L, Wu Y, Zeng G. Novel visiblelight-induced g-C₃N₄-Sb₂S₃/Sb₄O₅Cl₂ composite photocatalysts for efficient degradation of methyl orange. *Catal. Commun.* 2015; 70: 17-20.

[75] Lu X-C, Yang J-G, Zhang W-G, Huang Z. Improving the combustion and emissions of direct injection compression ignition engines using oxygenated fuel additives combined with a cetane number improver. *Energy Fuels* 2005;19:1879–88.

[76] Luque R, Budarin V, Clark JH, Macquarrie DJ. Glycerol transformations on polysaccharide derived mesoporous materials. *Appl Catal B*. 2008;82:157–62

[77] Machado M, Perez-Pariente J, Sastre E, Cardoso D, Guereñu M. Selective synthesis of glycerol monolaurate with zeolitic molecular sieves. *Appl Catal A: Gen* 2000;203:321–8.

[78] Mahajan D, Ganai BA, Sharma RL, Kapoor KK. Antimony chloride doped on hydroxyapatite catalyzed stereoselective one-pot synthesis of pyrano[3,2 c]quinolines. *Tetrahed Lett*. 2006; 47: 7919–21.

[79] Mallesham B, Sudarsanam P, Reddy BM. Production of Biofuel Additives from Esterification and Acetalization of Bioglycerol over SnO₂-Based Solid Acids. *Ind. Eng. Chem. Res.* 2014; 53, 18775–785.

[79] Manechakr P, Samerjit J, Uppakarnrod S, Karnjanakom S. Experimental design and kinetic study of ultrasonic assisted transesterification of waste cooking oil over sulfonated carbon catalyst derived from cyclodextrin. *J Ind Eng Chem.* 2015;32: 128–136.

[80] Mao D, Xia J, Zhang B, Lu G. Highly efficient synthesis of dimethyl ether from syngas over the admixed catalyst of CuO–ZnO–Al₂O₃ and antimony oxide modified HZSM-5 zeolite. *Energ Convers Manage* 2010; 51:1134–39.

[81] Melero JA, van Grieken R, Morales G, Paniagua M. Acidic mesoporous silica for the acetylation of glycerol: synthesis of bioadditives to petrol fuel. *Energy Fuels*. 2007;21:1782–91.

[82] Melero JA, van Grieken R, Morales G, Paniagua M. Acidic mesoporous silica for the acetylation of glycerol: synthesis of bioadditives to petrol fuel. *Energ Fuel* 2007; 21: 1782 –91.

- [83] Melero JA, Vicenta G, Paniagua M, Morales G, Munoz P, Etherification of biodiesel derived glycerol with ethanol for fuel formulation over sulfonic modified catalysts: *Bioresource technology*.2012;103:142-151.
- [84] Melero JA, Vicente G, Morales G. Acid-catalyzed etherification of bio-glycerol and isobutylene over sulfonic mesostructured silicas. *Appl Catal A* 2008;346:44-51.
- [85] Miller FA, Wilkins CH. Infrared Spectra and Characteristic Frequencies of Inorganic Ions Their Use in Qualitative Analysis. *Anal Chem* 1952; 8.
- [86] Mofijur M, Masjuki H, Kalam M, Shahabuddin M. Experimental study of additive added palm biodiesel in a compression ignition engine. *Energy Educ Sci Technol Part A: Energy Sci Res*. 2012;30:737-48.
- [87] Mori K, Hara T, Mizugaki T, Ebitani K, Kaneda K. Hydroxyapatite-Supported Palladium Nanoclusters: A Highly Active Heterogeneous Catalyst for Selective Oxidation of Alcohols by Use of Molecular Oxygen. *J. Am. Chem. Soc.* 2004;126 (34):10657–10666.
- [88] Murugan R, Rao KP, Kumar TSS. Heat-deproteinated xenogeneic bone from slaughter house waste: physico-chemical properties. *Bull. Mater. Sci.* 2003; 26: 528.
- [89] Nasr-Esfahani M, Fekri S. Alumina/TiO₂/hydroxyapatite interface nanostructure composite filters as efficient photocatalysts for the purification of air. *Reac Kinet Mech Cat.* 2012;107(1):89-103.
- [90] Nauss KM. Diesel Exhaust: A Critical Analysis of Emissions, Exposure, and Health Effects”, Health Effects Institute, Cambridge, MA, April 1995
- [91] Nouredini H, Daily WR, Hunt BA. Production of ethers of glycerol from crude glycerol-the by-product of biodiesel production. *Chem Biomol Eng Res.* 1998;13:121-9.

[92] Nripjit , Tyagi AK , Singh N. Characterization of Fabricated A 384.1-MgO Based Metal Matrix Composite and Optimization of Tensile Strength using Taguchi Techniques. *Materials and Metallurgical Engineering*.2012;6:8.

[93] Okumura K, Kobayashi Y, Hiraoka R, Dubois JL, Devaux JF. Process for preparing catalyst used in production of acrolein and/or acrylic acid and process for preparing acrolein and/or acrylic acid by dehydration reaction of glycerin. Patent WO2013008279 A1.

[94] Omid A, Habibi-Yangjeh A, Pirhashemi M. Application of ultrasonic irradiation method for preparation of ZnO nanostructures doped with Sb⁺³ ions as a highly efficient photocatalyst. *Appl Surf Sci* 2013; 276: 468-75.

[95] Oner C, Altun S. Biodiesel production from inedible animal tallow and an experimental investigation of its use as alternative fuel in a direct injection diesel engine. *Appl Energy*. 2009;86: 2114–20.

[96] Oprescu E-E, Dragomir RE , Radu E, Radu A, Velea S, Bolocan I, Stepan E, Rosca P. Performance and emission characteristics of diesel engine powered with diesel–glycerol derivatives blends. *Fuel Process Technol*. 2014;126: 460–468.

[97] Pagliaro M, Ciriminna R, Kimura H, Rossi M, Pina CD, *Angew. Chem. Int. Ed.*, 2007, 46,2–20, *Angew. Chem*. 2007, 119(24), 4516-4522.

[98] Paliagro M, Rossi M. The future of glycerol: new uses of a versatile raw material. *RSC Green Chem* 2008;5:212-8.

[99] Pan C, Li Y, Ma Y, Zhao X, Zhang Q. Platinum-antimony doped tin oxide nanoparticles supported on carbon black as anode catalysts for direct methanol fuel cells. *J.Power Source*. 2011;196:6228-6231.

[100] Pandi K, Viswanathan N. Synthesis of alginate bio encapsulated nano-hydroxyapatite composite for selective fluoride sorption. *Carbohydrate Polymers*. 2014;112(0):662-7.

[101] Park MS, Vislovskiy VP, Chang JS, Shul YG, Yooet. Al. Catalytic dehydrogenation of ethylbenzene with carbon dioxide: promotional effect of antimony in supported vanadium–antimony oxide catalyst. *Cat Today* 2003; 87:205-12.

[102] Patel A, Singh S. A green and sustainable approach for esterification of glycerol using 12-tungstophosphoric acid anchored to different supports: Kinetics and effect of support. *Fuel* 118 (2014) 358–364.

[103] Potty A, Xenopolous A. Removal of protein aggregates from biopharmaceutical preparations using calcium phosphate salts. US Patent 2011/0301333.

[104] Pradhan P, Chakraborty R. Fly ash supported Ni-Fe solid acid catalyst for efficient production of diesel additive: intensification through far-infrared radiation. *Asia Pac. J. Chem. Eng.* 2016; 11: 4-6.

[105] Pradhan P, Chakraborty S, Chakraborty R. Optimization of infrared radiated fast and energy-efficient biodiesel production from waste mustard oil catalyzed by Amberlyst 15: Engine performance and emission quality assessments. 2016;173:60–68.

[106] Pramanik T, Tripathi S. Biodiesel: clean fuel of the future. *Hydrocarbon Process*. 2005;84:49-54.

[107] Prasad L, Pradhan S, Das LM, Naik SN. Experimental assessment of toxic phorbol ester in oil, biodiesel and seed cake of *Jatropha curcas* and use of biodiesel in diesel engine. *Appl Energ* 2012; 93:245–50.

- [108] Rahmat N, Abdullah AZ, Mohamed AR. Recent progress on innovative and potential technologies for glycerol transformation into fuel additives: a critical review. *Renew Sust Energy Rev* 2010; 14:987–1000.
- [109] Rakopoulos CD, Rakopoulos DC, Hountalas DT, Giakoumis EG, Andritsakis EC. Performance and emissions of bus engine using blends of diesel fuel with biodiesel of sunflower or cottonseed oils derived from Greek feedstock. *Fuel* 2008;87:147-57.
- [110] Rastegari H, Ghaziaskar HS, Yalpani M. Valorization of Biodiesel Derived Glycerol to Acetins by Continuous Esterification in Acetic Acid: Focusing on High Selectivity to Diacetin and Triacetin with No Byproducts. *Ind. Eng. Chem. Res.* 2015; 54: 3279-84.
- [111] Rehman I, Bonfield W. Characterization of hydroxyapatite and carbonated apatite by photo acoustic FTIR spectroscopy. *J. Mater. Sci. Mater. Med.* 1997; 8:1-4.
- [112] Ribeiro NM, Pinto AC, Quintella CM. The role of additives for diesel and diesel blended (ethanol or biodiesel) fuels: a review. *Energy Fuels.* 2007;21:2433-45.
- [113] Saka S, Isayama Y. A new process for catalyst-free production of biodiesel using supercritical methyl acetate. *Fuel* 2009; 88: 1307–13.
- [114] Sakthivel A, Nakamura R, Komura K, Sugi Y. Esterification of glycerol by lauric acid over aluminium and zirconium containing mesoporous molecular sieves in supercritical carbon dioxide medium. *J Supercrit Fluids* 2007;42:219-25.
- [115] Sakthivel G, Nagarajan G, Ilangkumaran M, Gaikwad AB. Comparative analysis of performance, emission and combustion parameters of diesel engine fuelled with ethyl ester of fish oil and its diesel blends. *Fuel.* 2014;132:116–124.

- [116] Sanosh, KP, Chu MC, Balakrishnan A, Kin TN, Cho SJ. Utilization of bio waste eggshells to synthesize nanocrystalline hydroxyapatite. *Mater. Lett.* 2009; 63: 2100.
- [117] Schober S, Mittelbach M. The impact of antioxidants on biodiesel oxidation stability. *Eur J Lipid Sci Technol.* 2004;106:382–9.
- [118] Sebti S, Tahir R, Nazih R, Boulaaja S. Comparison of different Lewis acid supported on hydroxyapatite as new catalysts of Friedel–Crafts alkylation. *Appl. Catal., A.*2001;218: 25–30.
- [119] Sebti S, Tahir R, Nazih R, Saber A, Boulaajaj S. Hydroxyapatite as a new solid support for the Knoevenagel reaction in heterogeneous media without solvent. *Appl. Catal., A.*2002;228: 155–159.
- [120] Sharma G, Sharma MP. Impact of cold flow properties of bio diesel on engine performance: *Renewable and sustainable energy review.* 2014;31: 650-656.
- [121] Silitonga AS, Masjuki HH, Mahlia TMI, Ong HC, Chong WT, Boosroh MH. Overview properties of biodiesel diesel blends from edible and non-edible feedstock. *Renew Sustain Energy Rev.* 2013;22:346–60.
- [122] Singh D, Patidar D, Ganesh P, Mahajan A, Esterification of oleic acid with glycerol in presence of supported zinc oxide as catalyst. *Chem. Res.* 2013;52:14776-14786.
- [123] Singh S, Patel A. Selective Green Esterification and Oxidation of Glycerol over 12 Tungstophosphoric Acid Anchored to MCM-48. *Ind. Eng. Chem. Res* 2014; 53:14592-600.
- [124] Smith C. Biodiesel revolution gathering momentum; 2004, <http://www.straight.com/print/3568> [accessed January 8, 2009].
- [125] Sobczak-Kupiec A, Wzorek Z The influence of calcination parameters on free calcium oxide content in natural hydroxyapatite. *Ceram Int* 2012; 38: 641–47.

- [126] Sun J, Tong X, Yu L, Wan J. An efficient and sustainable production of triacetin from the acetylation of glycerol using magnetic solid acid catalysts under mild conditions. *Catal Today* 2016; 264: 115-22
- [127] Ullman TL, Spreen KB, Mason RL. Effects of cetane number, cetane improver, aromatics, and oxygenates on heavy-duty diesel engine emissions. *SAE Technical Paper*; 1994.
- [128] Vedaraman N, Puhan S, Nagarajan G, Velappan K. Preparation of palm oil biodiesel and effect of various additives on NO_x emission reduction in B20: an experimental study. *Int J Green Energy*. 2011;8:383–97.
- [129] Venkateshwarlu G, Rajanna KC, Saiprakash PK. Antimony Trioxide as an Efficient Lewis Acid Catalyst for the Synthesis of 5- Substituted 1H-Tetrazoles. *Synth. Commun: An International Journal for Rapid Communication of Synthetic Organic Chemistry*. 2009; 39: 426-32.
- [130] Venugopal A, Scurril MS. Hydroxyapatite as a novel support for gold and ruthenium catalysts Behaviour in the water gas shift reaction. . *Appl. Catal., A*.2003;245:137–147.
- [131] Votsmeier M, Kreuzer T, Lepperhoff G. Automobile Exhaust control, *Ullmann's Encyclopedia of Industrial Chemistry*. 2005
- [132] Wang S, Guin JA, Xinhe B, Yide X. Synthesis of gasoline additives from methanol and olefins over sulfated silica. *Stud Surf Sci Catal*. 2004;439-44.
- [133] Xiong HM, Chen JS, Li DM. Controlled growth of Sb₂O₅ nanoparticles and their use as polymer electrolyte fillers. *J. Mater. Chem.*, 2003; 13: 1994 – 98
- [134] Yang H, Hu Y, Qiu G. Preparation of antimony doped SnO₂ nanocrystallites. *Mater Res Bull* 2002; 37: 2453-58.

- [135] Yazdani SS, Gonzalez R. Anaerobic fermentation of glycerol: a path to economic viability for the biofuels industry. *Curr Opin Biotechnol.* 2007;18:213-9.
- [136] Yilmaz N, Vigil FM, Benalil K, Davis SM, Calva A. Effect of biodiesel–butanol fuel blends on emissions and performance characteristics of a diesel engine. *Fuel.*2014;135:46–50.
- [137] Zahouily M, Abrouki Y, B. Bahlaouan, A. Rayadh S. Sebti. Hydroxyapatite: new efficient catalyst for the Michael addition. *Catal commun.* 2003;4: 521–524.
- [138] Zhang ZH, Liu YH. Antimony trichloride/SiO₂ promoted synthesis of 9-ary-3,4,5,6,7,9-hexahydroxanthene-1,8-diones. *Cat Commun* 2008; 9: 1715-19.
- [139] Zhang, H., Ying, P., Zhang, J., Liang, C., Feng, Z. & Li, C. SbO_x/SiO₂ catalysts for the selective oxidation of methane to formaldehyde using molecular oxygen as oxidant, In: *Studies in Surface Science and Catalysis*, X. Bao and Y. Xu, Eds, (Natural Gas Conversion VII.2004;147:547-552.
- [140] Zhou L, Nguyen TH, Adesina AA. The acetylation of glycerol over amberlyst-15: Kinetic and product distribution. *Fuel Process. Technol.* 2012; 104: 310–18.
- [141] Zhu S, Gao X, Dong F, Zhu Y, Zheng H, Li Y. Design of a highly active silver-exchanged phosphotungstic acid catalyst for glycerol esterification with acetic acid. *J. Catal.* 2013; 306: 155–163.
- [142] Federal Report. National Air Toxics Program: The Integrated Urban Strategy”, Notice, 64 FR 38706, July 19, 1999.
- [143] <http://www.chevron.com/products/oronite/products/fuel-additives.html>.

APPENDIX I:

ABBREVIATIONS:

TA	Triacetin
XRD	Xray diffraction
EHA	Ethyl hexyl acetate
DT	Diacetin & Triacetin
SSA	Specific surface area
KOH	Potassium hydroxide
NHAp	Natural hydroxylapatite
TOLM	Taguchi orthogonal L ₉ matrix
SSP	Solid state polycondensation
TGA	Thermogravimetric analysis
SEM	Scanning electron microscopy
BET	Brunauer Emmett and Teller
BSFC	Brake specific fuel consumption
EGT	Exhaust gas temperature
BTE	Brake thermal efficiency
CHBR	Conventionally heated batch reactor
IRRABR	Infrared radiation aided batch reactor
GC-MS	Gas chromatography mass spectroscopy
ESP	Experimentally synthesized product
FTIR	Fourier transform infrared spectroscopy

APPENDIX II:

LIST OF FIGURES:

Fig. 2.1: Increasing production of biodiesel and crude glycerol lead to plummeting glycerol price.....	11
Fig. 2.2: Industry wise application of glycerol.....	12
Fig. 6.1 Individual Plot representing parametric effects.....	43
Fig. 6.2 Contour Plot showing parameter interaction & DT yield.....	44
Fig. 6.3 Effect of a. AA:G mole ratio and b. Reaction Temperature on G conversion and ester yield (at optimal condition).....	45
Fig 6.4. Effect of a. catalyst concentration, b. Sb precursor loading, Reaction time c. for IRRABR and d. for CHBR on glycerol conversion, diacetin and triacetin yield.....	47
Fig. 6.5. TGA Analyses of NHAp and SH 4 samples.....	49
Fig. 6.6. FTIR analyses of Sb_PHAp catalyst.....	50
Fig. 6.7. XRD analyses of Sb_PHAp catalyst.....	52
Fig. 6.8. SEM Micrograph of a. dried SH 4 and b. calcined SH 4.....	54
Fig. 6.9. SH 4 catalyst reusability in esterification of G with AA.....	55
Fig. 6.10. Probable Reaction Mechanism for esterification of G with AA.....	55
Fig. 6.11. Engine emission values for different test fuels.....	58
Fig. 6.12. Exhaust emission characteristics for palm biodiesel based diesel engine at different speed for a. CO b. CO ₂	59

Fig. 6.13. Exhaust emission characteristics for palm biodiesel based diesel engine at different speed for a. HC and b. NOx.....	60
Fig. 6.14. Engine Performance Analysis for different test fuels.....	61
Fig. 6.15. Engine performace for palm biodiesel blends and neat biodiesel at different speed for a. Brake Specific Fuel Consumption b. Brake Thermal Efficiency.....	63
Fig. 6.16. Engine performace for palm biodiesel blends and neat biodiesel at different speed for c. Heat Input and d. Exhaust Gas Temperature.....	64
Fig. 6.17. Effect of additive on different biodiesel blends a. Flash Point b. Pour Point.....	66
Fig. 6.18. Effect of additive on biodiesel property a. Cetane number b. Density.....	67
Fig. 6.19. Effect of additive on biodiesel property a. Viscosity b. Acid value.....	68
Fig. 6.20. Exhaust emission variation with engine speed fuelled with blended biodiesel in diesel engine for a. CO emission b. CO ₂ emission.....	70
Fig. 6.21. Exhaust emission variation with engine speed fuelled with blended biodiesel in diesel engine for a. NOx emission b. HC emission.....	71
Fig. 6.22. Engine performace of diesel engine fuelled by palm biodiesel blends and neat biodiesel at different speed for a. Brake Specific Fuel Consumption b. Brake Thermal Efficiency and c. Exhaust Gas Temperature.....	73

APPENDIX III:

LIST OF TABLES:

Table 2.1: Physical properties of diesel.....	6
Table 2.2: Diesel Emission Constituents and their impact.....	6
Table 2.3: Physical Properties of biodiesel.....	8
Table 2.4: Fuel property comparison between diesel and biodiesel.....	13
Table 2.5: Glycerol based additives.....	14
Table 3.1: Glycerol based fuel additives.....	18
Table 3.2: Glycerol based fuel additives (Continued).....	20
Table 3.2: Application of Hydroxylapatite (HAp) as a Catalyst & Catalyst Support.....	27
Table 3.4: Application of Hydroxylapatite (HAp) as a Catalyst & Catalyst Support (Continued).....	28
Table 3.5: Cetane Number of fatty esters (<i>Knothe et al., 2003</i>).....	33
Table 5.1: TOLM at different parametric conditions showing corresponding DT yield (Y_{DT}) and SN ratios.....	38
Table 6.1: Analysis of variance for DT Yield.....	42
Table 6.2: Response Table for Signal to Noise (SN) ratio.....	43
Table 6.3: Effect of IR activation and different catalysts on DT selectivity (Eq. 4).....	48
Table 6.4: BET Surface Area and Product Distribution.....	53
Table 6.5: Effect of commercial Triacetin and Experimental Product application on Palm Biodiesel...	56

10. RESEARCH ACTIVITY

Communicated Journal Paper

1. A full length paper entitled “**Pork bone supported Sb Catalyst for Glycerol Acetic Acid Esterification under Infrared Excitation for Fuel Additive Synthesis: Engine Performance and Exhaust Analysis**” has been communicated to *Energy Conversion and Management* (Elsevier) 2016.

Conference Attended

2. Presented paper entitled “**Assessment of 2- Ethyl hexyl acetate as Biodiesel Additive: Property evaluation and Engine Performance Analyses**” at 5th International Conference on Advances in Energy Research at Indian Institute of Technology, Bombay (ICAER 2015).